Supporting Information.

Ag^+-induced reverse vesicle to helical fiber transformation in a self-assembly by tinkering around the keto-enol equilibrium of a chiral salicylideneaniline

Sougata Datta,[a] and Santanu Bhattacharya[*ab]
[a]Department of Organic Chemistry, Indian Institute of Science, Bangalore 560 012, India
[b]Jawaharlal Nehru Centre for Advanced Scientific Research, Bangalore 560 064, Jakkur, India
E-mail: sb@orgchem.iisc.ernet.in

Table of contents: **Page no.**

(a) Physical Measurements and Instrumentation.

Gelation Experiment. A weighed amount of compound **1** was added into 1 ml toluene or benzene in a sealed glass vial and warmed briefly to afford a cloudy suspension. To that suspension 0.5 equiv. of $AgSO_3CF_3$ pre-dissolved in ethanol was added which was followed by vortexing for 'homogeneous' mixing (toluene:ethanol = 100:1). Then, the resulting mixture was incubated at room temperature for 5 min to check the stability of the gel using inverse flow method.[1,2] Whenever, a gel was formed, it was evaluated quantitatively by determining the minimum gelator concentration (MGC) which is defined as the minimum amount of gelator required to immobilize 1 mL of a particular solvent. Each of the experiments was performed at least in duplicate to ensure reproducibility.

^{1}H-NMR Spectroscopy. ^{1}H-NMR spectra of **1** and its Ag^+-coordination complex were recorded on a Bruker-400 Avance NMR spectrometer using C_6D_6 in the presence of 1% CD_3OD (v/v) as the solvent.

UV-Vis and Circular Dichroism Spectroscopy. The UV-Vis spectroscopy and circular dichroism spectroscopy of the samples were recorded on a Shimadzu 2100 UV-Vis spectrophotometer, and on JASCO J-815 spectrometer respectively.

Raman Spectroscopy. Raman spectra of the samples were recorded with a Raman spectrometer (Renishaw inVia model). A 785 nm laser diode of 300 mW was used as an excitation source.

Scanning Electron Microscopy (SEM). The toluene solution of **1** and the gel sample of the corresponding Ag^+-coordination complex were carefully drop cast onto brass stubs and were allowed to freeze-dry overnight. The samples were then coated with gold vapor and analyzed on a Quanta 200 SEM operated at 15 kV.

Atomic Force Microscopy (AFM). AFM images were obtained by using JPK model AFM instrument and analyzed by Nano Wizard JPK00901 software. The toluene solution of **1** and the gel sample of the corresponding Ag^+-coordination complex were deposited directly on flat, freshly cleaved mica substrates and dried in ambient air for 24 h. AFM images were captured in the tapping mode.

Transmission Electron Microscopy (TEM). 10 μL of each sample in toluene was drop-coated onto a carbon-coated copper grid (300 mesh size) and allowed to air-dry at room temperature. Then 10 μL of an aqueous 0.1% uranyl acetate solution was drop-coated on the sample placed on the grid and allowed to stand for 24 h. TEM images were taken at an accelerating voltage of 100 and 200 kV using a TECNAI F30.

Dynamic Light Scattering (DLS). Size of the spherical aggregates present in the toluene sol of compound **1** was measured on a Zetasizer Nano ZS90, Malvern.

Hydrophobic Dye Encapsulation in Reverse Vesicle and Fluoresence Microscopic Studies. 1 mg of compound **1** was added to a toluene solution of Nile red (0.5 mL, 0.39 mM) taken in a sample vial followed by sonication for 15 min. The final concentrations were 3.9 mM for compound **1** and 0.39 mM for Nile red. The resultant mixture was placed in a dialysis bag (molecular weight cutoff = 1000 Da) and dialyzed against toluene for 72 h. The outside toluene was replaced every 6 h interval to remove any free dye. The toluene solution left in the dialysis bag contained only Nile red encapsulated reverse vesicles of **1**, which was further observed under a fluorescence microscope (OLIMPUS IX-81) at 20× magnification.

Small-angle and Wide-angle X-ray Diffraction (SAXD and WAXD). The toluene gel and solution were scooped and drop-coated respectively onto glass slide and dried under vacuum for the corresponding XRD measurements. SAXD and WAXD measurements were performed on a PANalytical-EMPYREAN-SAXS and Philips-X'Pert-PANalytical-XRD instrument respectively, using the X-ray beam generated with rotating Cu anode at the wavelength of Kα beam at 1.5418Å.

Electrochemical Measurements. Cyclic voltammetry experiments were carried out in CHI645D, CH instrument with a conventional three-electrode cell (solution volume of 5 mL). A teflon stopper (provided with holes for insertion of the electrodes) was used as a tight cover to exclude atmospheric oxygen. The working electrode was a glassy carbon electrode with a geometrical area of 0.07 cm^2 and mounted in Teflon. The electrode was polished before each experiment with 0.3 μm alumina pastes followed by extensive rinsing with ultrapure Milli-Q water. Platinum wire was used as the counter electrode and saturated calomel electrode, SCE, as reference electrode. 0.1 (M) n-$Bu_4N^+PF_6^-$ toluene-acetonitrile (5:1) solution was used as the supporting electrolyte and was routinely deoxygenated by argon bubbling. All potential values are given versus the calomel saturated electrode SCE. Cyclic voltammetry experiments were conducted within the potential range of -0.5 to -1.3 V at the scan rate of 0.1 V s^{-1}.

(b) Materials and Methods. All chemicals, solvents and silica gel for TLC and column chromatography were obtained from well-known commercial sources and were used without further purification, as appropriate. Solvents were distilled and dried by standard procedure before use. Melting points were measured in open capillaries and were uncorrected. FT-IR studies were performed on a Perkin-Elmer FT-IR Spectrometer BX model by incorporating the samples in KBr disk and were reported in wave numbers (cm^{-1}). ^{1}H-NMR and ^{13}C-NMR spectra were recorded Bruker-400 Avance NMR spectrometer at 400

and 100 MHz respectively. Chemical shifts were reported in ppm downfield from the internal standard tetramethylsilane (TMS). Elemental analysis was recorded in Thermo Finnigan EA FLASH 1112 SERIES.

(c) Scheme S1.[a]

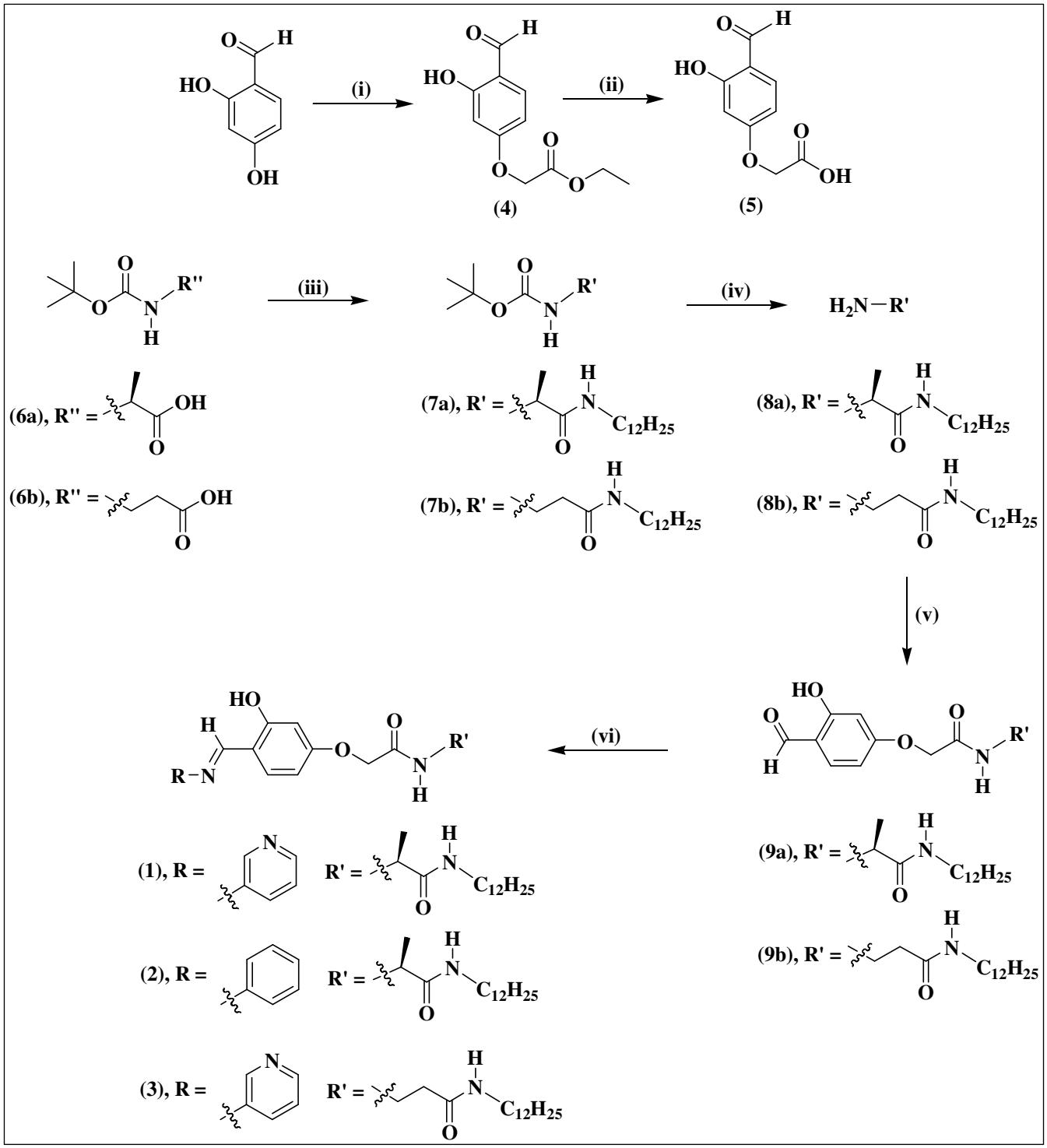

[a] (i) $NaHCO_3$, dry DMF, ethyl bromoacetate, 70 °C, 48 h, yield = 70%; (ii) aq. NaOH (1M)/EtOH (1:1), reflux at 80 °C, 3 h, yield = quantitative; (iii) *n*-$C_{12}H_{25}NH_2$, DCC, DMAP, HOBT, CH_2Cl_2, rt, 12 h, yield = 80% (**7a**), 85% (**7b**); (iv) TFA, CH_2Cl_2, rt, 6 h, yield = quantitative (**8a-b**); (v) **5**, DCC, DMAP, pyridine, CH_2Cl_2, 0 °C to rt, 24 h, yield = 70% (**9a**), 65% (**9b**); (vi) 3-aminopyridine or aniline, ethanol, reflux, 80 °C, 6 h, yield = 85% (**1**), 90% (**2**), 80% (**3**).

(d) Synthetic procedure and characterization data.

Synthesis. Compounds **1-3** were synthesized according to the reaction scheme 1 and were characterized by FTIR, ^{1}H-NMR, ^{13}C-NMR spectroscopy and mass spectrometry (ESI-MS) and elemental analysis. Compound **4**, **5**, **6**, **7** and **8** were prepared as described earlier.[1-3]

General procedure for the synthesis of 9a-b. Compound **8** (1 g, 3.89 mmol) and 4-formyl-3-hydroxyphenoxyacetic acid (**5**) (0.764 g, 3.89 mmol) were dissolved in dry CH_2Cl_2 (30 ml) containing dry pyridine (0.47 ml, 5.85 mmol). The solution was cooled to 0 °C. Catalytic amount of DMAP (0.047 g, 0.389 mmol) and DCC (0.965 g, 4.68 mmol) were added to the mixture and stirred for 24 h at room temperature. White precipitate of DCU was removed by filtration. The filtrate was diluted with CH_2Cl_2. The organic layer was washed with 2N HCl and water. After drying over anhyd. Na_2SO_4, solvent was evaporated under reduced pressure and the resultant residue was purified by column chromatography (petroleum ether/ EtOAc = 4:1) on silica gel to get a white solid.

Compound 9a. Yield: 70%; IR (KBr): 3283, 3091, 2921, 2851, 1769, 1711, 1674, 1646, 1628, 1567, 1500, 1435, 1381, 1365, 1347 cm^{-1}; ESI-MS: m/z 457.2750 $[M + Na]^+$; ^{1}H-NMR (400 MHz, $CDCl_3$, TMS, rt): δ (ppm) 0.87 (t, 3H, *J* = 6.8 Hz), 1.25-1.29 (m, 18H), 1.43-1.52 (m, 5H), 3.22-3.28 (m, 2H), 4.49-4.58 (m, 3H), 6.03 (s, 1H), 6.46 (s, 1H), 6.63-6.64 (m, 1H), 7.18 (d, 1H, *J* = 6.8 Hz), 7.5 (d, 1H, *J* = 8.4 Hz), 9.76 (s, 1H), 11.44 (s, 1H); ^{13}C-NMR (100 MHz, $CDCl_3$, TMS, rt): δ (ppm) 13.96, 18.25, 22.53, 24.77, 25.45, 26.68, 29.09, 29.19, 29.29, 29.34, 29.38, 29.40, 29.43, 29.48, 31.76, 33.74, 39.37, 48.39, 65.02, 101.35, 108.38, 115.69, 135.3, 161.68, 164.15, 167.15, 171.85, 194.41; Elemental analysis: calcd. for $C_{24}H_{38}N_2O_5$: C, 66.33; H, 8.81; N, 6.45; Found: C, 66.35; H, 8.79; N, 6.46.

Compound 9b. Yield: 65%; IR (KBr): 3322, 3090, 2923, 2852, 1759, 1710, 1674, 1646, 1628, 1564, 1506, 1445, 1376, 1336 cm^{-1}; ESI-MS: m/z 457.2725 $[M + Na]^+$; ^{1}H-NMR (400 MHz, $CDCl_3$, TMS, rt): δ (ppm) 0.88 (t, 3H, *J* = 6.8 Hz), 1.26-1.31 (m, 18H), 1.51 (d, 2H, *J* = 8.8 Hz), 2.45 (t, 2H, *J* = 5.6 Hz), 3.23-3.28 (m, 2H), 3.61-3.65 (m, 2H), 4.11 (s, 2H), 5.56 (s, 1H), 6.39 (s, 1H), 6.59 (d, 1H, *J* = 8.8 Hz), 6.88-7.01 (m, 1H), 7.46 (d, 1H, *J* = 8.8 Hz), 9.74 (s, 1H), 11.43 (s, 1H); ^{13}C-NMR (100 MHz, $CDCl_3$, TMS, rt): δ (ppm) 14.09, 22.69, 24.96, 25.66, 26.28, 26.91, 29.26, 29.34, 29.52, 29.58, 29.63, 29.64, 31.02, 31.93, 32.8, 33.98, 35.87, 39.77, 49.25, 67.62, 101.77, 108.38, 115.93, 135.5, 164.32, 164.98, 167.7, 170.95, 194.51; Elemental analysis: calcd. for $C_{24}H_{38}N_2O_5$: C, 66.33; H, 8.81; N, 6.45; Found: C, 66.34; H, 8.80; N, 6.44.

General procedure for the synthesis of salicylideneaniline derivatives (1-3). A solution of the compound **9** (0.434 g, 0.1 mmol) and the corresponding amine (0.1 mmol) in ethanol was heated to reflux

for 3 h and cooled to room temperature. The precipitate was collected by filtration and washed using *n*-hexane thoroughly to obtain a solid product.

Compound 1. Yield: 85%; mp = 172-173 ºC; IR (KBr): 3569, 3513, 3421, 3289, 3091, 2920, 2851, 1698, 1656, 1626, 1565, 1467, 1437, 1362, 1343 cm^{-1}; ESI-MS: m/z 533.31 $[M + Na]^+$; ^{1}H-NMR (400 MHz, $CDCl_3$, TMS, rt): δ (ppm) 0.87 (t, 3H, *J* = 6.8 Hz), 1.24-1.29 (m, 18H), 1.43-1.52 (m, 5H), 3.22-3.28 (m, 2H), 4.5-4.58 (m, 3H), 6.12 (s, 1H), 6.55-6.63 (m, 2H), 7.19 (d, 1H, *J* = 7.6 Hz), 7.38 (d, 2H, *J* = 8.4 Hz), 7.57 (d, 1H, *J* = 8.4 Hz), 8.51-8.57 (m, 3H), 13.23 (s, 1H); ^{13}C-NMR (100 MHz, $CDCl_3$, TMS, rt): δ (ppm) 14.03, 18.31, 22.61, 24.86, 25.54, 26.78, 29.19, 29.27, 29.38, 29.46, 29.51, 29.56, 31.83, 33.86, 39.67, 48.48, 66.97, 102.19, 107.4, 114, 123.84, 127.93, 134.19, 142.89, 144.59, 147.57, 161.4, 163.25, 163.45, 167.17, 171.29; Elemental analysis: calcd. for $C_{29}H_{42}N_4O_4$: C, 68.21; H, 8.29; N, 10.97; Found: C, 68.23; H, 8.27; N, 10.98.

Compound 2. Yield: 90%. mp = 164-165 ºC; IR (KBr): 3568, 3294, 3083, 2956, 2921, 2852, 1642, 1400 cm^{-1}; ESI-MS: m/z 532.32 $[M + Na]^+$; ^{1}H-NMR (400 MHz, $CDCl_3$, TMS, rt): δ (ppm) 0.89 (t, 3H, *J* = 6.8 Hz), 1.26-1.29 (m, 18H), 1.44-1.53 (m, 5H), 3.24-3.29 (m, 2H), 4.51-4.59 (m, 3H), 6.02 (s, 1H), 6.55-6.59 (m, 2H), 7.13 (d, 1H, *J* = 7.6 Hz), 7.27-7.29 (m, 3H), 7.34 (d, 1H, *J* = 8.4 Hz), 7.43 (t, 2H, *J* = 8.4 Hz), 8.57 (s, 1H) 13.83 (s, 1H); ^{13}C-NMR (100 MHz, $CDCl_3$, TMS, rt): δ (ppm) 14.06, 18.18, 22.64, 26.81, 29.21, 29.29, 29.42, 29.49, 29.53, 29.58, 31.86, 39.69, 48.5, 66.99, 102.22, 106.99, 114.25, 120.99, 126.65, 129.38, 133.8, 148.13, 160.96, 161.3, 163.84, 167.4, 171.26; Elemental analysis: calcd. for $C_{30}H_{43}N_3O_4$: C, 70.7; H, 8.50; N, 8.24; Found: C, 70.72; H, 8.51; N, 8.23.

Compound 3. Yield: 80%. mp = 168-171 ºC; IR (KBr): 3565, 3525, 3416, 3324, 3252, 3091, 2922, 2851, 1712, 1656, 1624, 1561, 1400, 1379 cm^{-1}; ESI-MS: m/z 511.328 $[M + H]^+$; ^{1}H-NMR (400 MHz, $CDCl_3$, TMS, rt): δ (ppm) 0.88 (t, 3H, *J* = 6.4 Hz), 1.26-1.37 (m, 18H), 1.50 (t, 2H, *J* = 6.4 Hz), 2.45 (t, 2H, *J* = 6 Hz), 3.23-3.28 (m, 2H), 3.61-3.65 (m, 2H), 4.09 (s, 2H), 5.61 (s, 1H), 6.49-6.58 (m, 2H), 7.06-7.09 (m, 1H), 7.33-7.37 (m, 2H), 7.56 (d, 1H, *J* = 8 Hz), 8.5-8.56 (m, 3H), 13.19 (s, 1H); ^{13}C-NMR (100 MHz, $CDCl_3$, TMS, rt): δ (ppm) 14.09, 22.67, 24.96, 25.66, 26.91, 29.26, 29.34, 29.52, 29.56, 29.58, 29.63, 29.64, 31.92, 33.98, 35.87, 39.76, 49.22, 67.71, 102.14, 107.55, 113.82, 123.87, 127.91, 134.15, 140, 143.09, 147.62, 162.59, 163.4, 163.48, 170.96; Elemental analysis: calcd. for $C_{29}H_{42}N_4O_4$: C, 68.21; H, 8.29; N, 10.97; Found: C, 68.19; H, 8.27; N, 10.96.

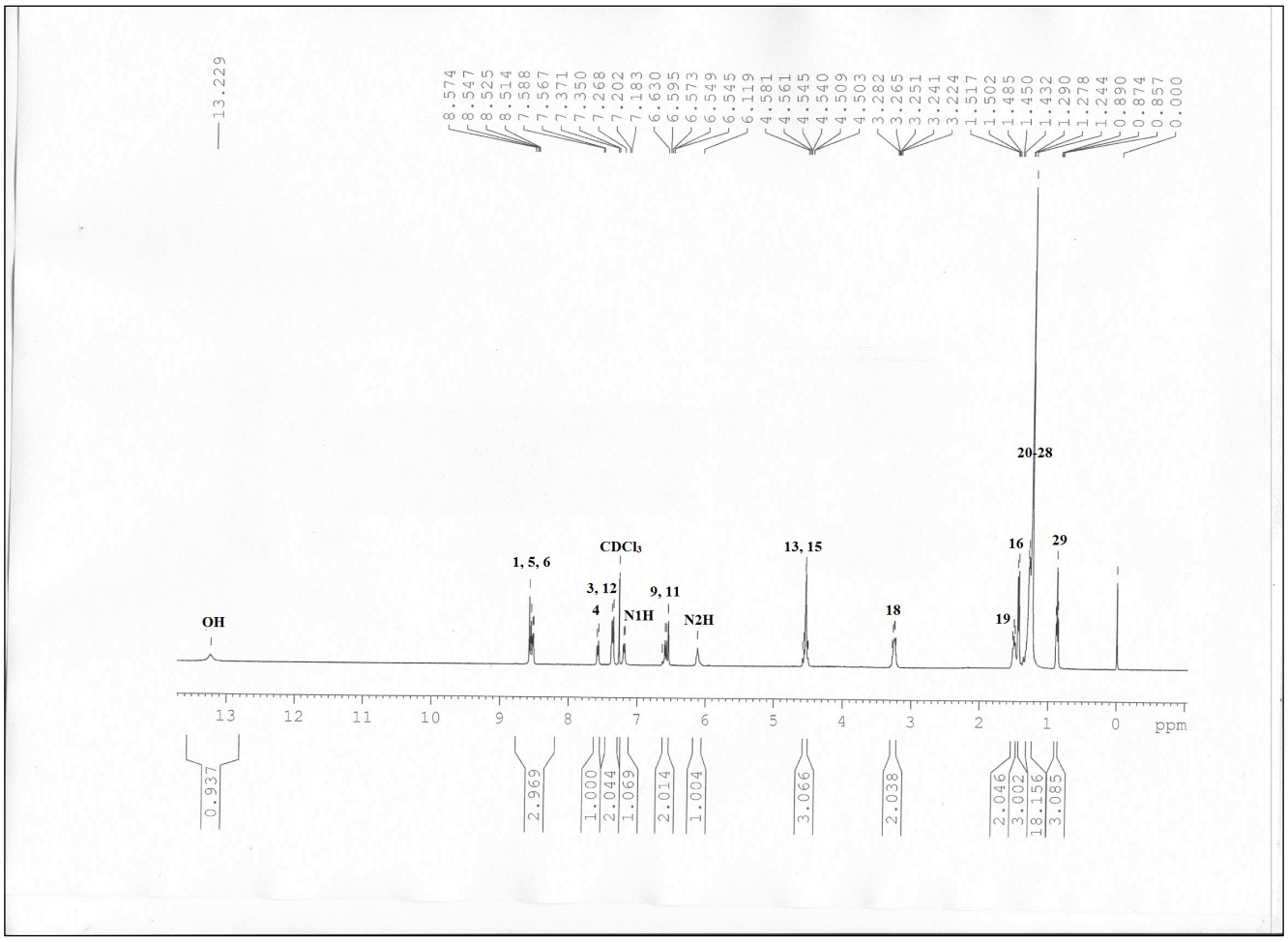

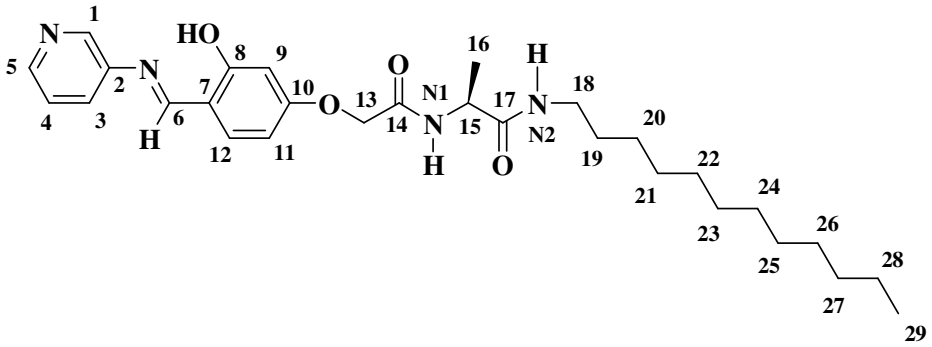

Figure S1. [1]H-NMR spectrum of compound **1**.

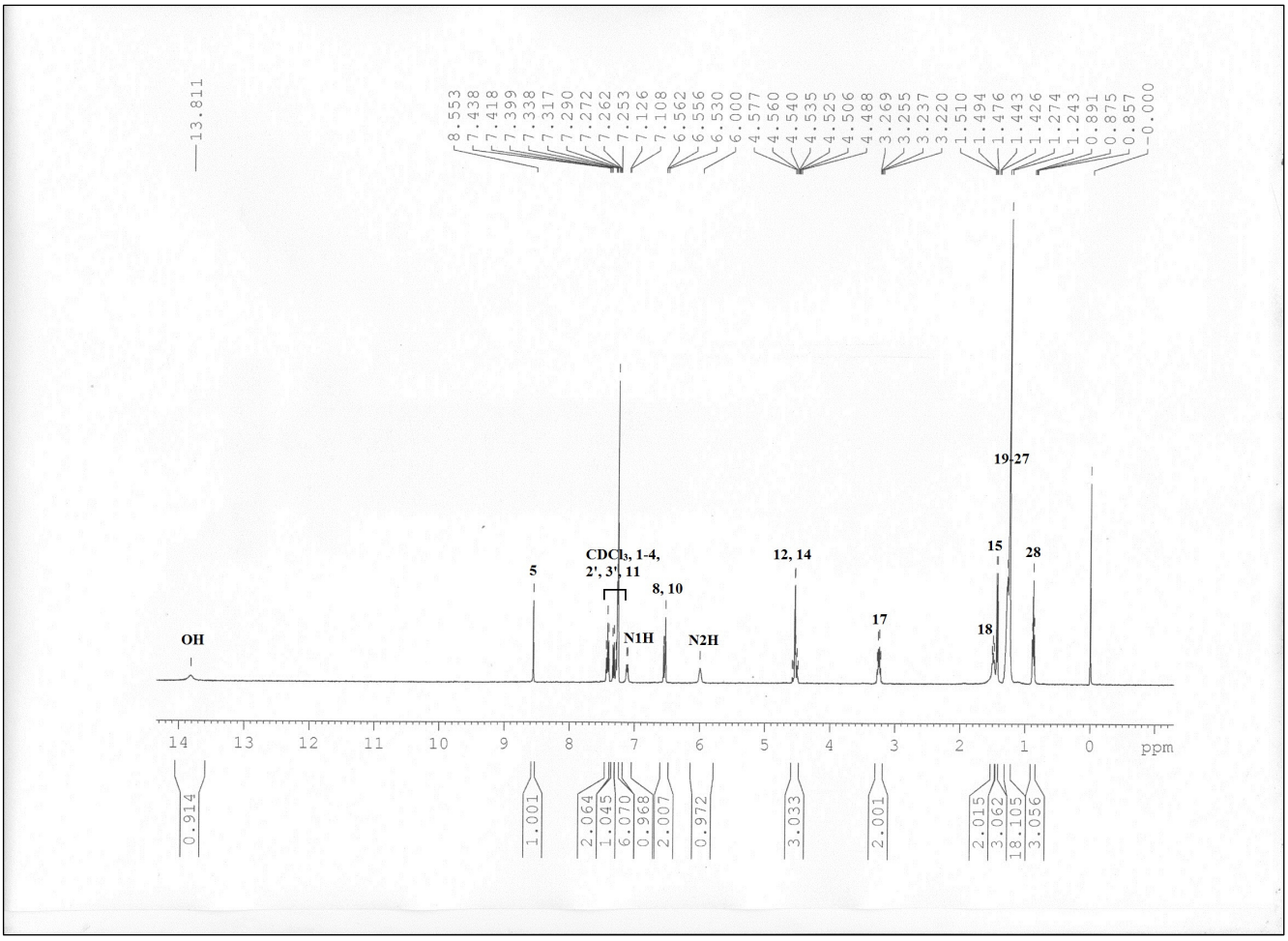

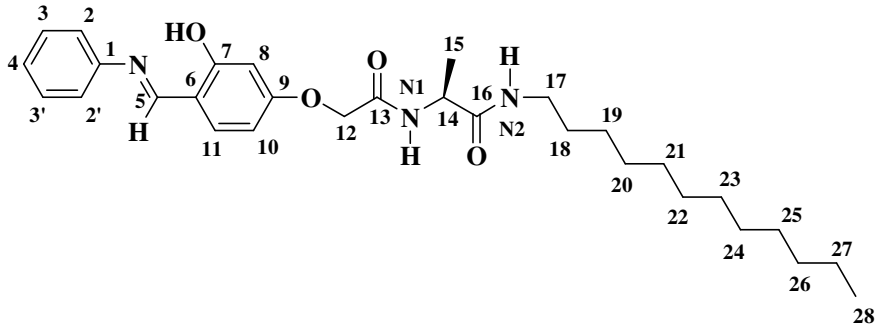

Figure S2. [1]H-NMR spectrum of compound **2**.

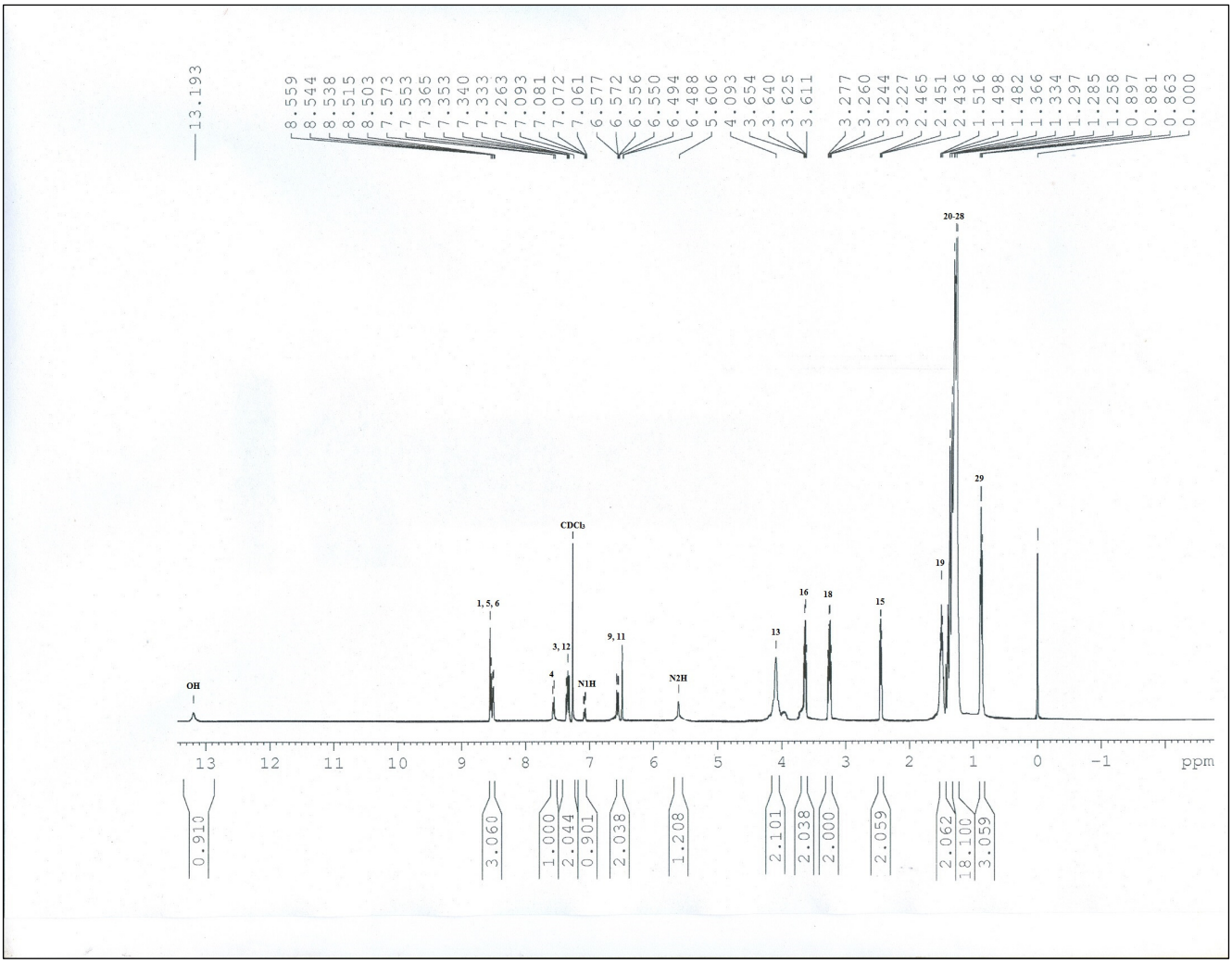

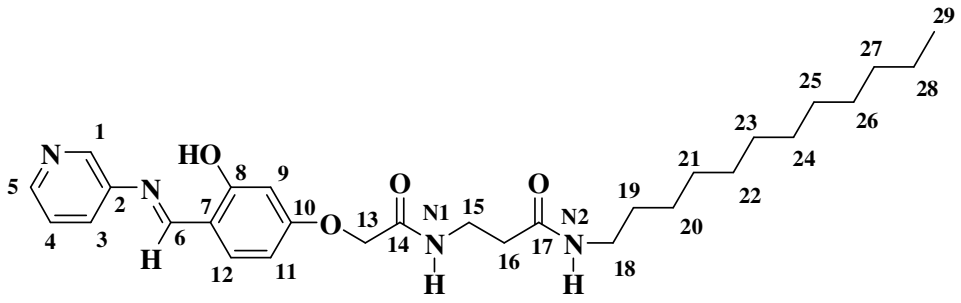

Figure S3. [1]H-NMR spectrum of compound **3**.

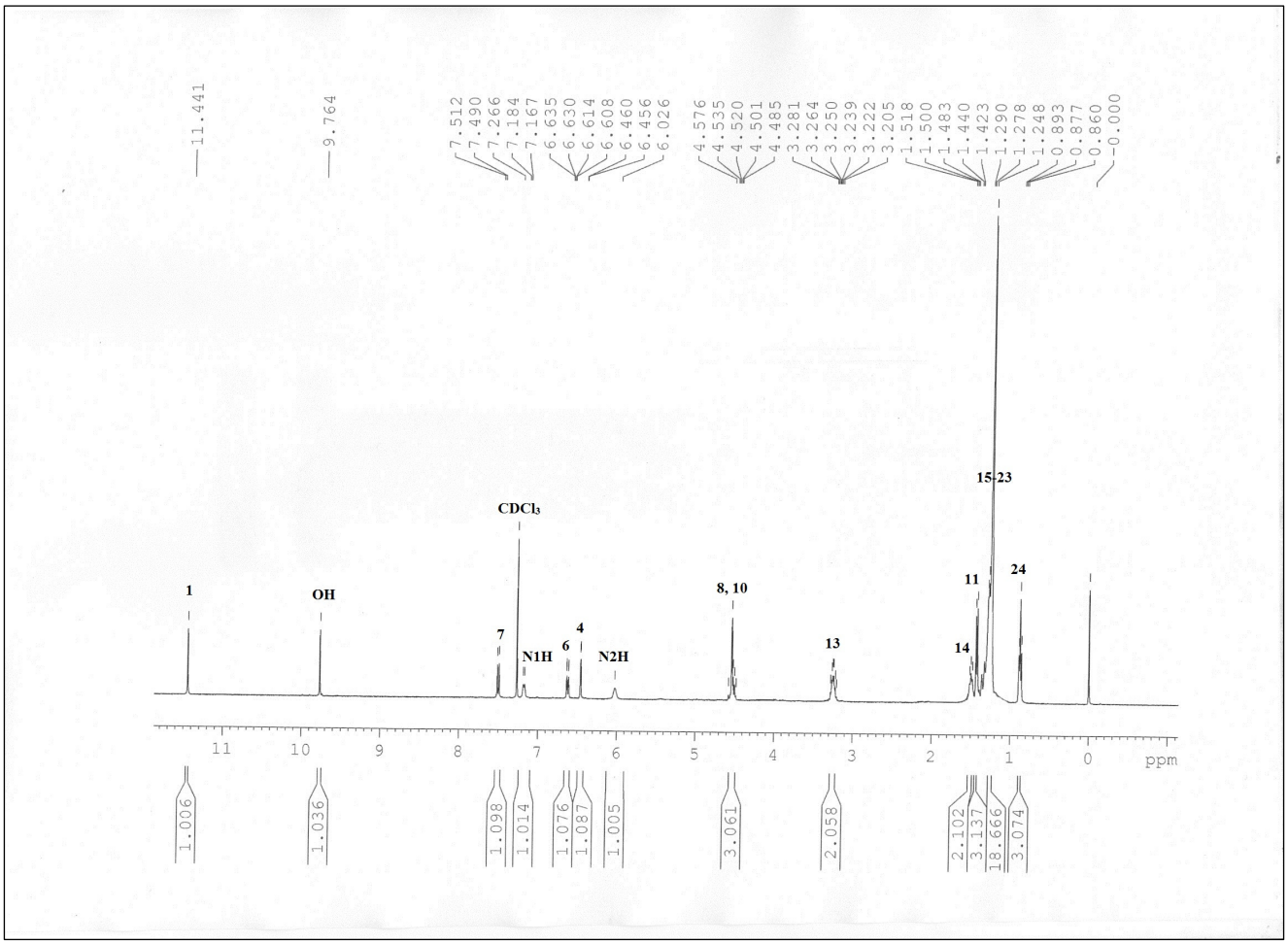

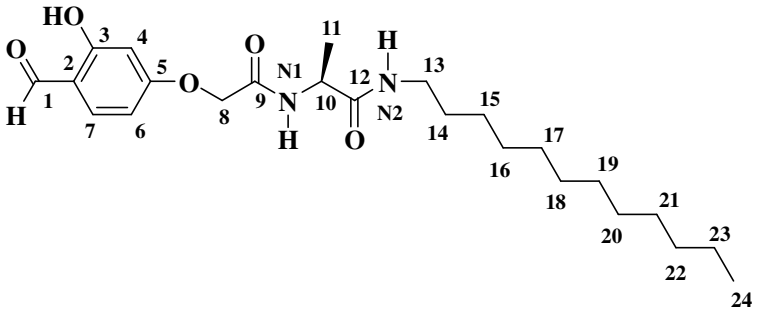

Figure S4. [1]H-NMR spectrum of compound **9a**.

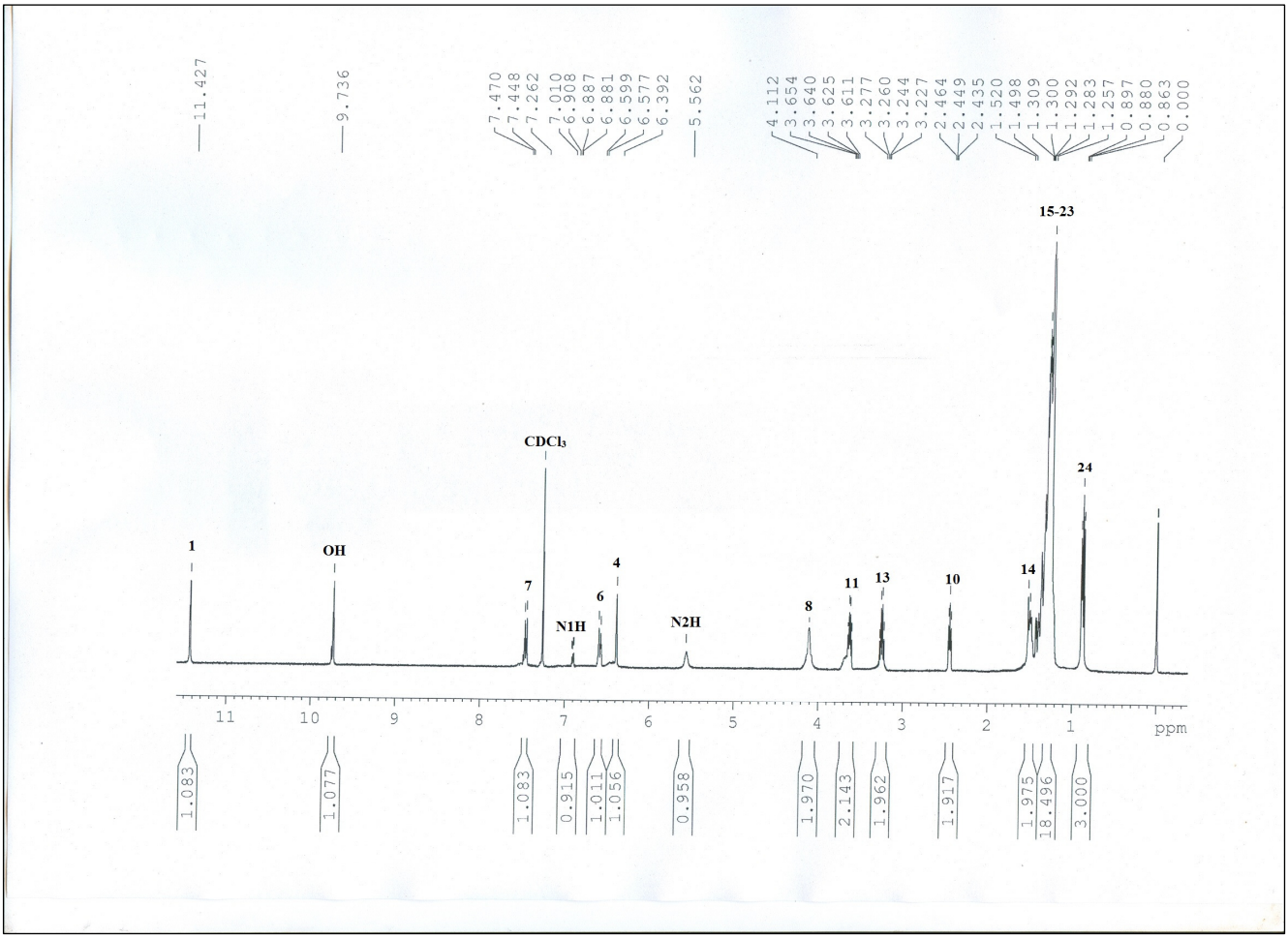

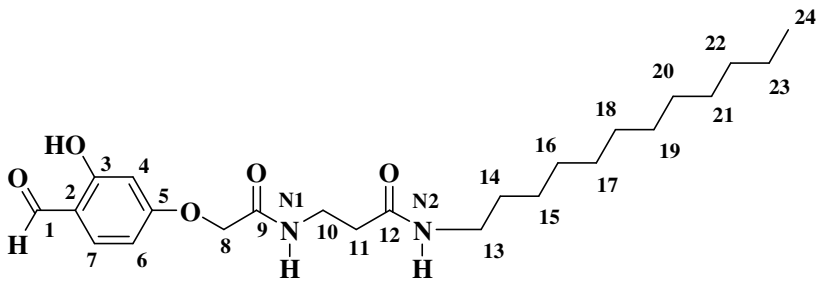

Figure S5. [1]H-NMR spectrum of compound **9b**.

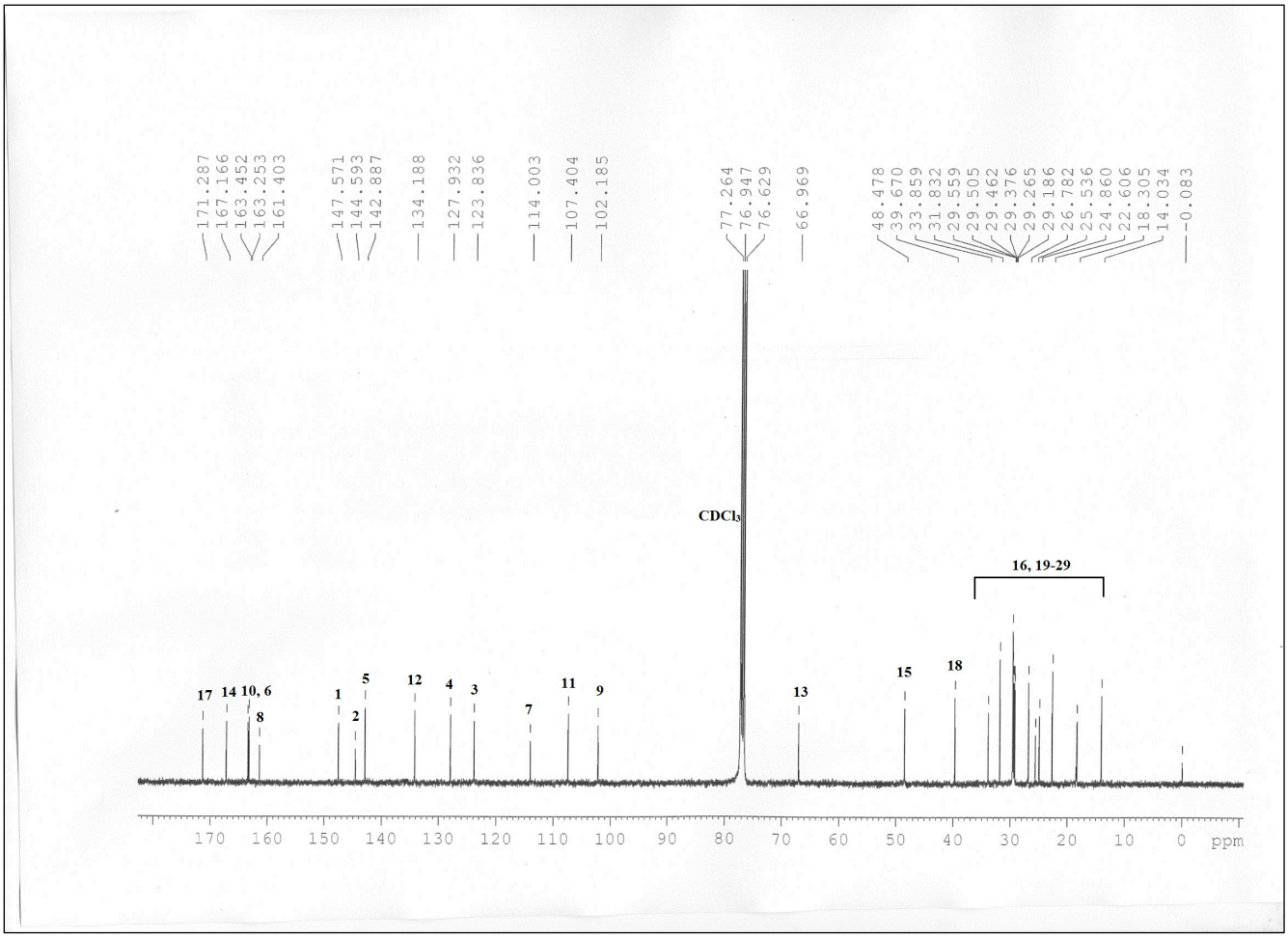

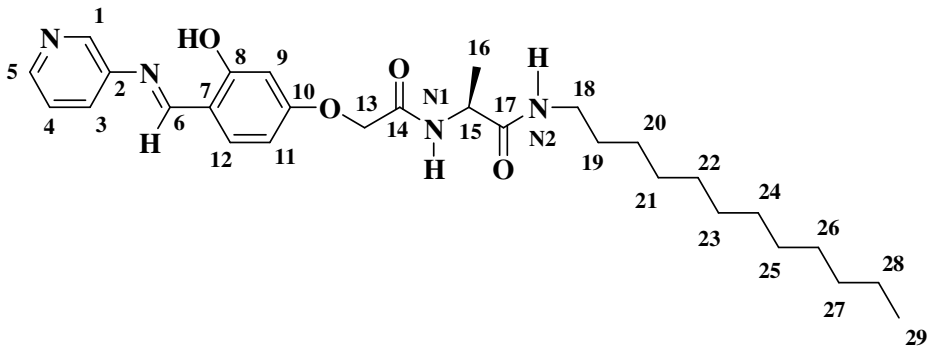

Figure S6. ^{13}C-NMR spectrum of compound **1**.

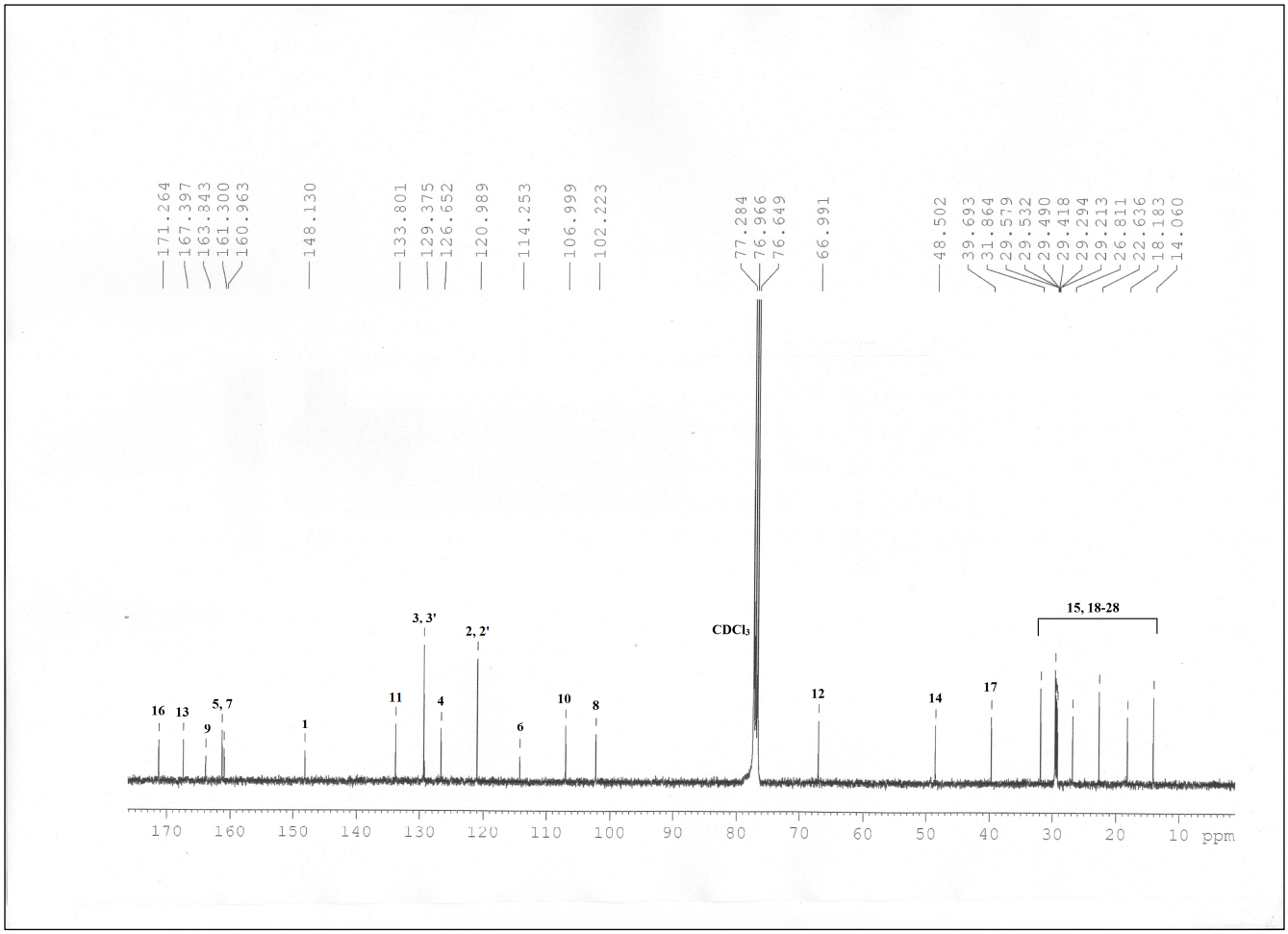

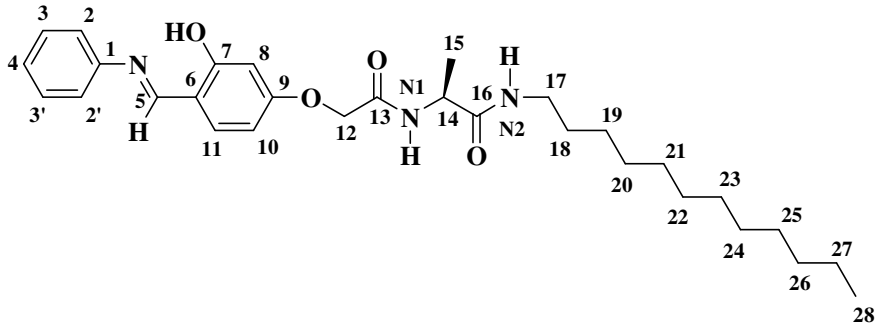

Figure S7. ^{13}C-NMR spectrum of compound **2**.

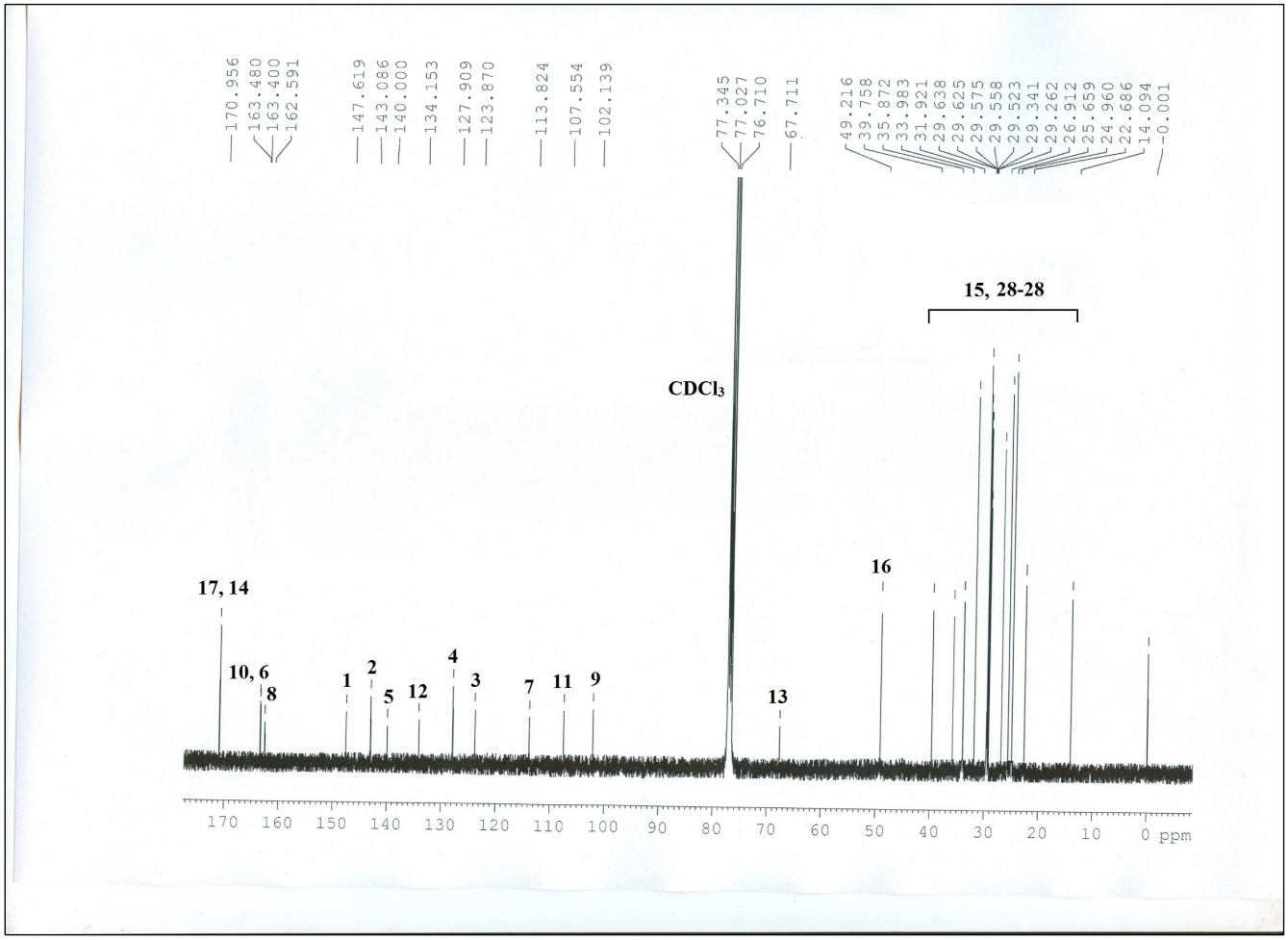

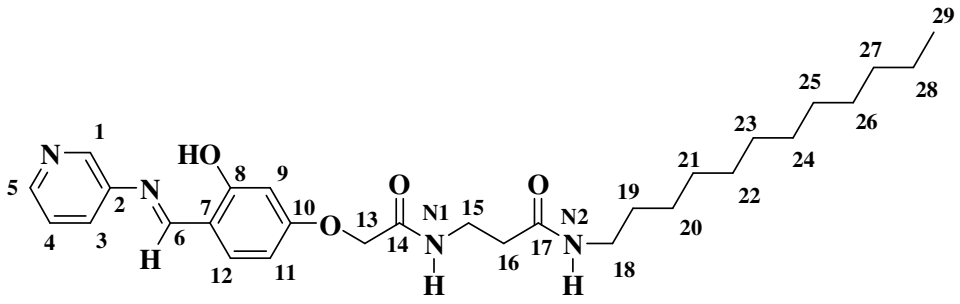

Figure S8. ^{13}C-NMR spectrum of compound **3**.

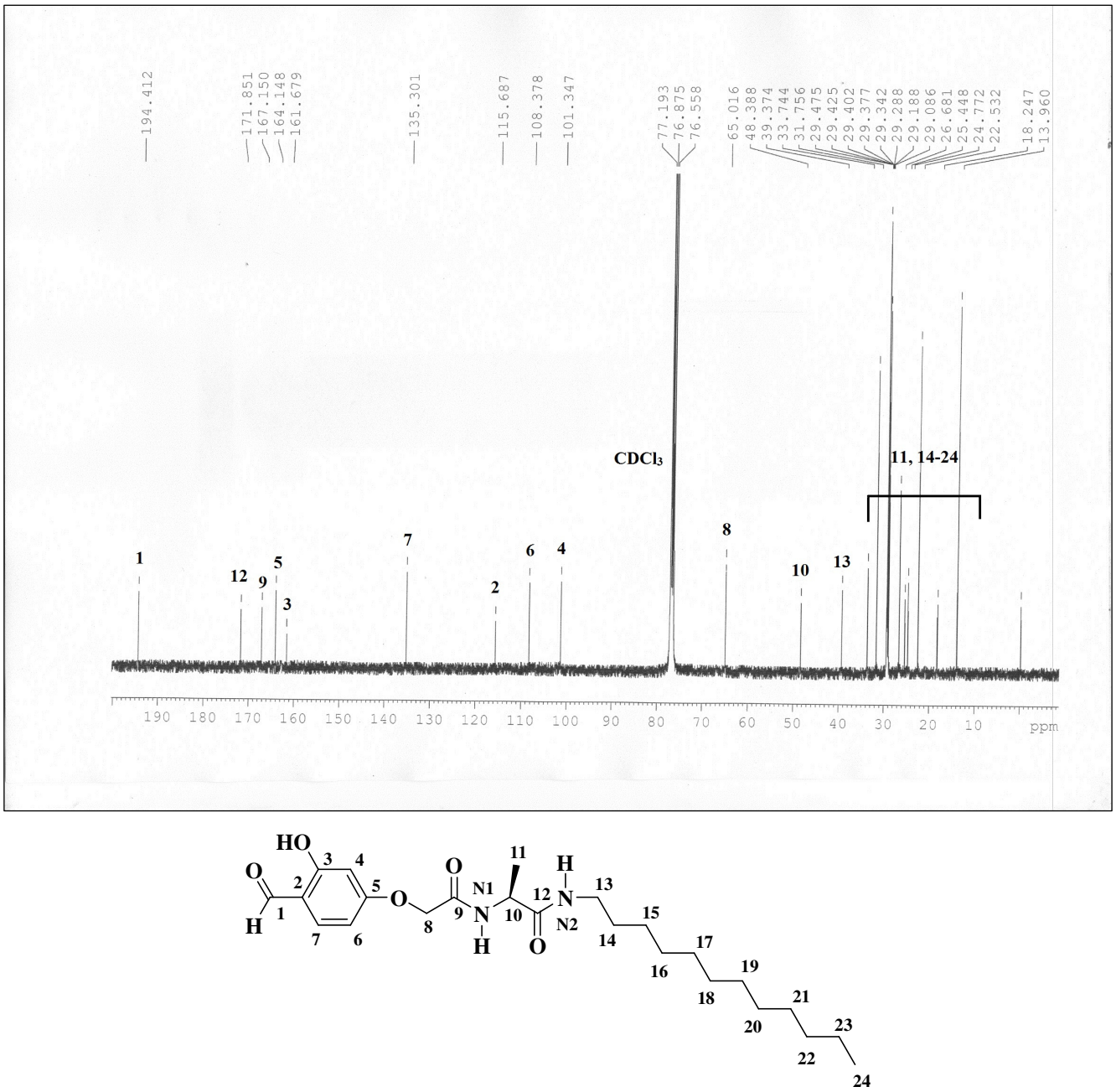

Figure S9. ^{13}C-NMR spectrum of compound **9a**.

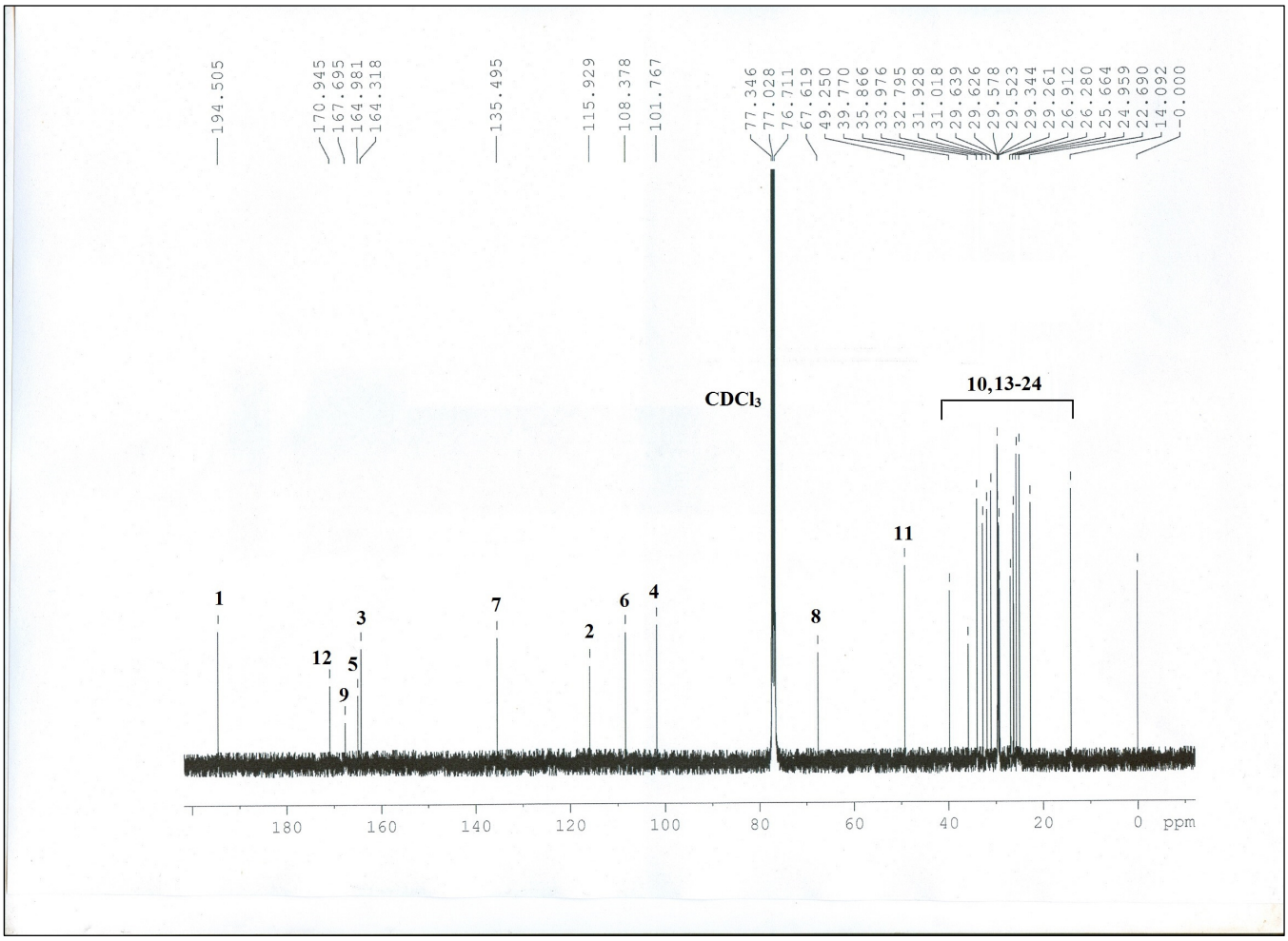

Figure S10. ^{13}C-NMR spectrum of compound **9b**.

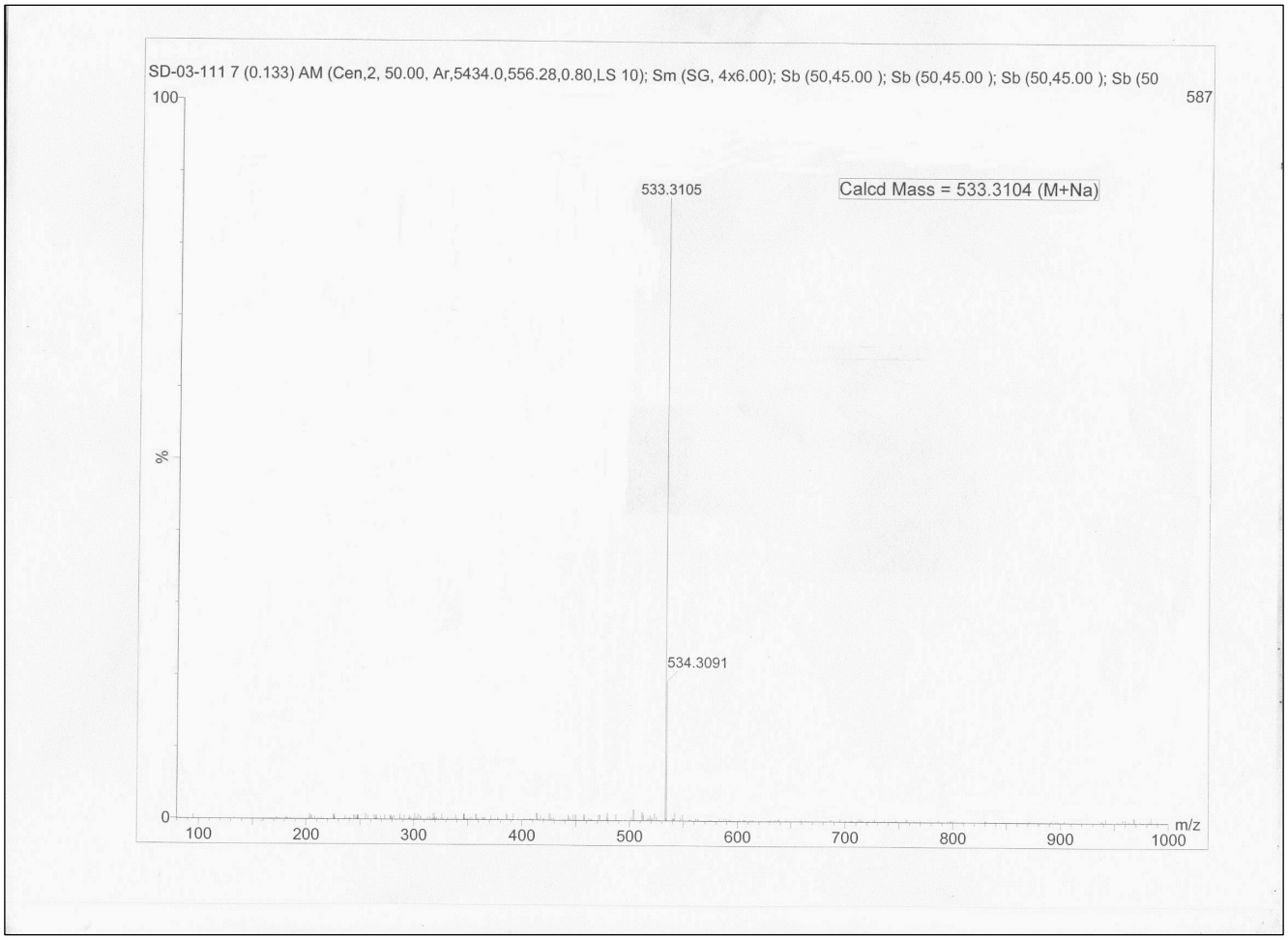

Figure S11. High resolution mass spectrum of compound **1**.

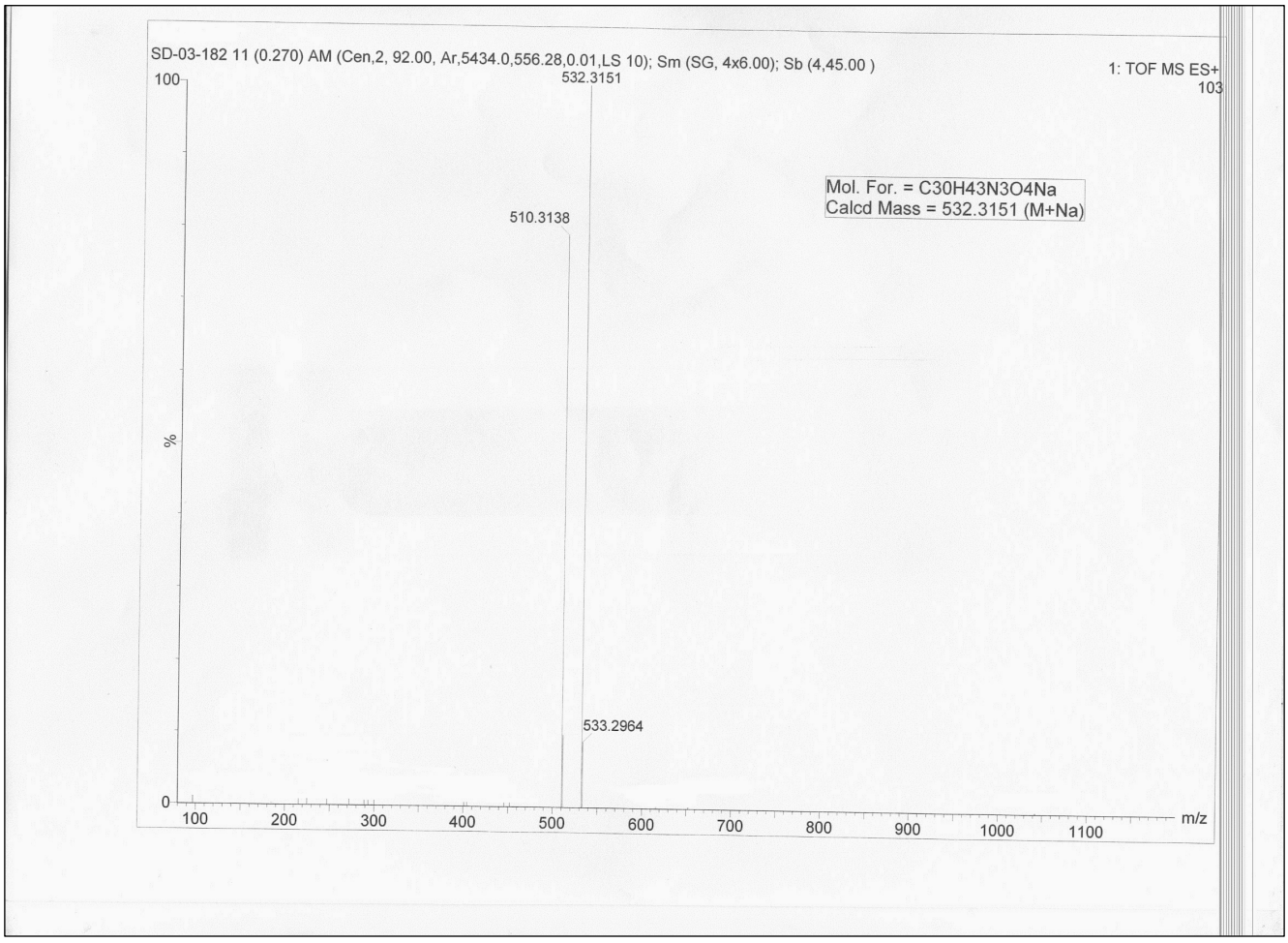

Figure S12. High resolution mass spectrum of compound **2**.

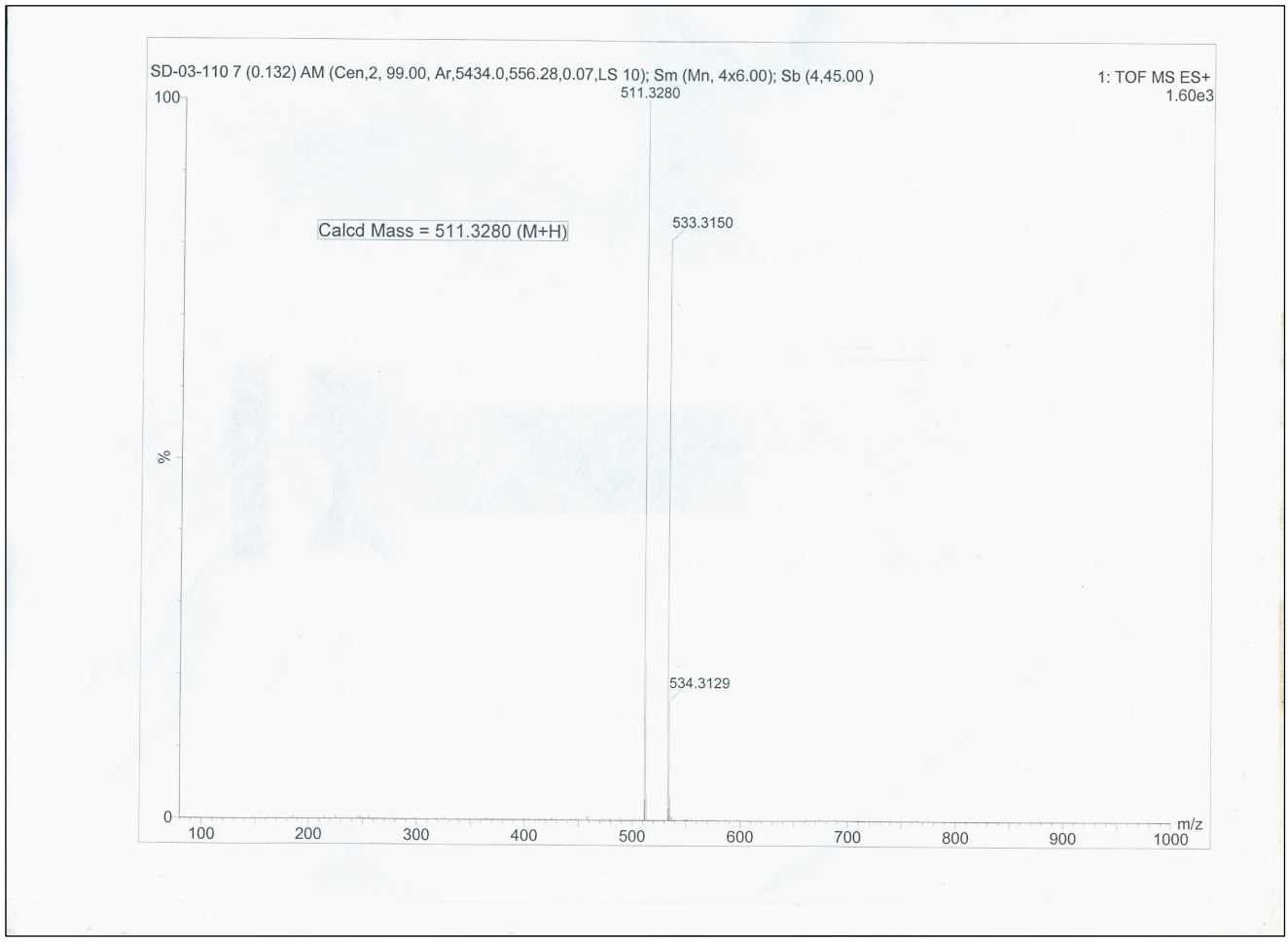

Figure S13. High resolution mass spectrum of compound **3**.

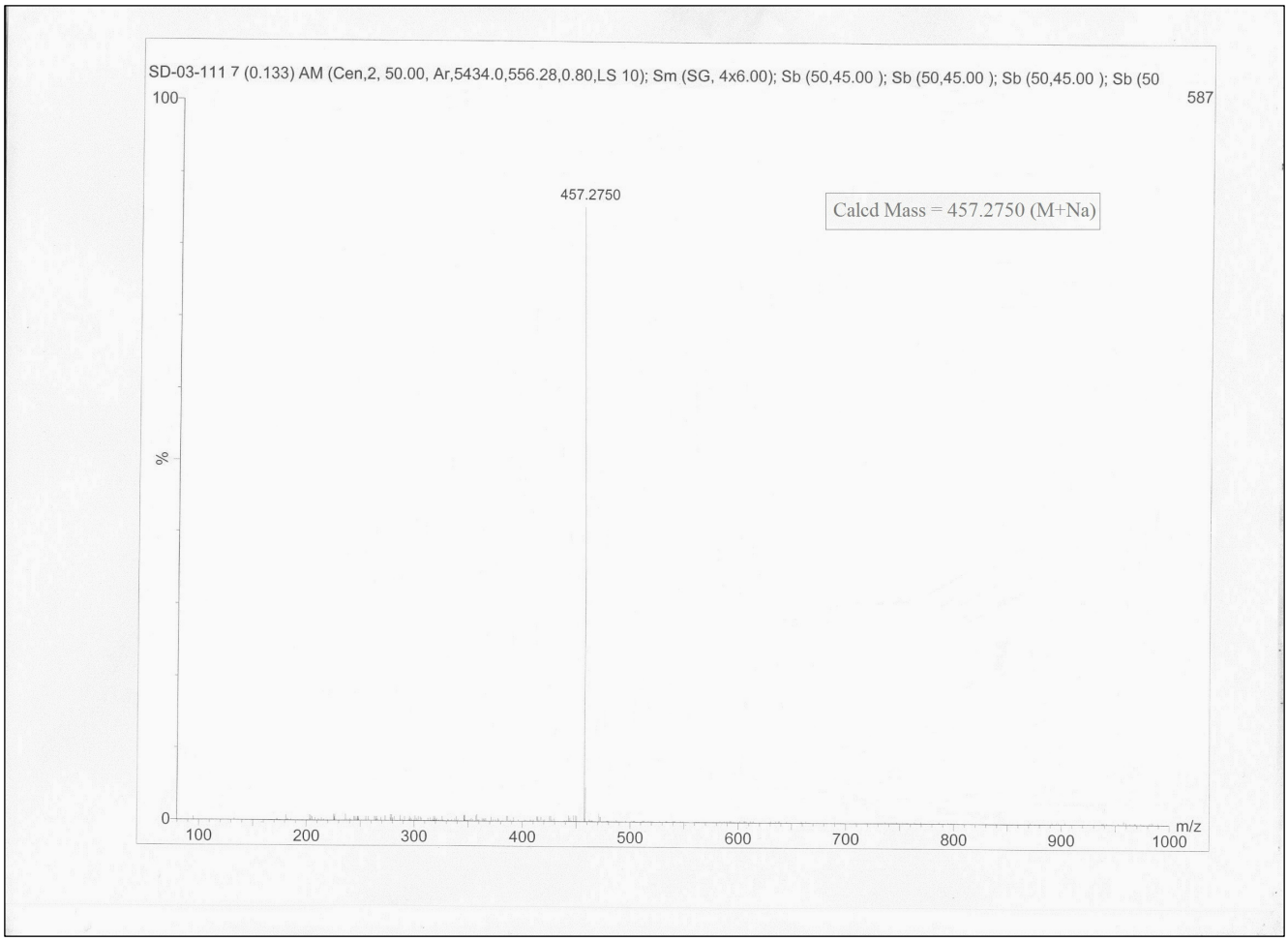

Figure S14. High resolution mass spectrum of compound **9a**.

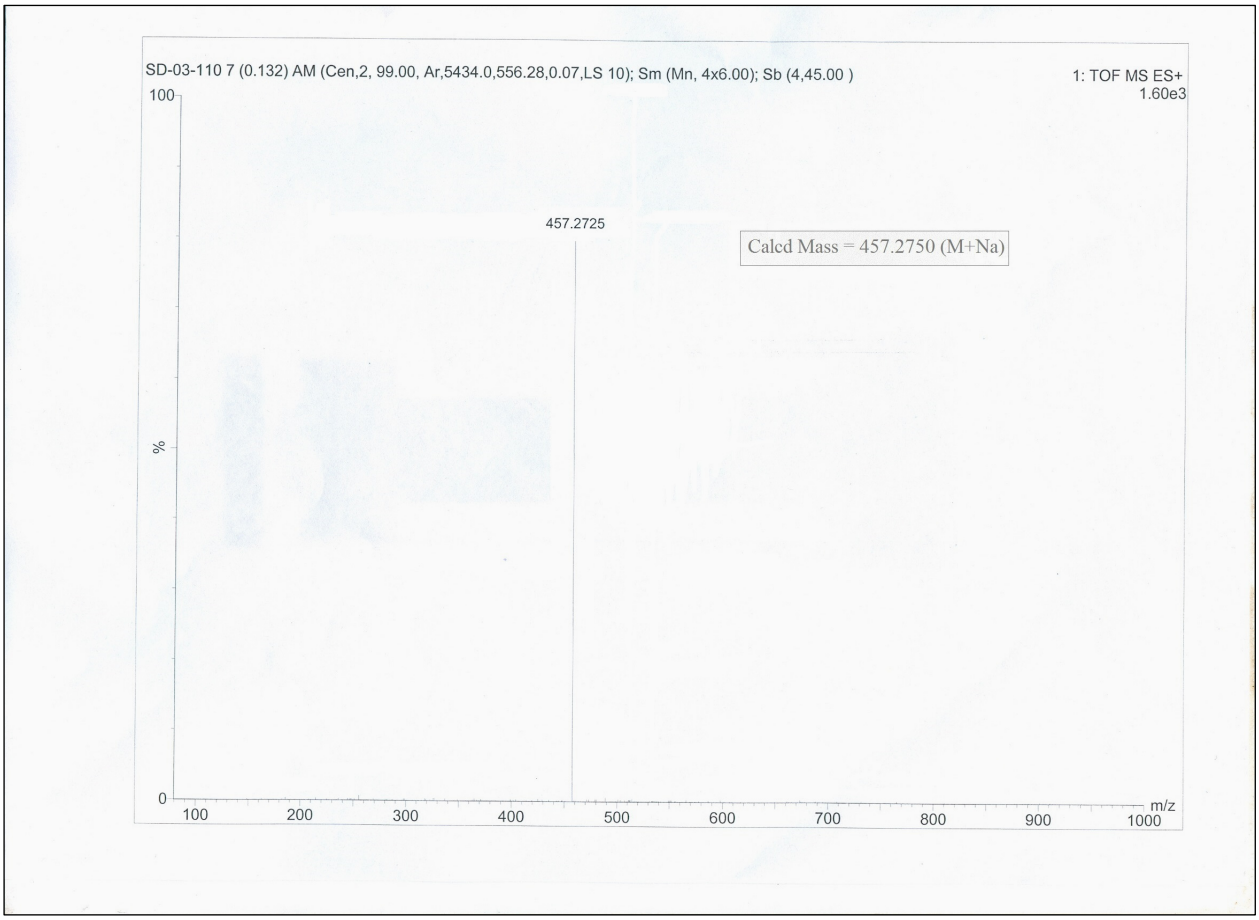

Figure S15. High resolution mass spectrum of compound **9b**.

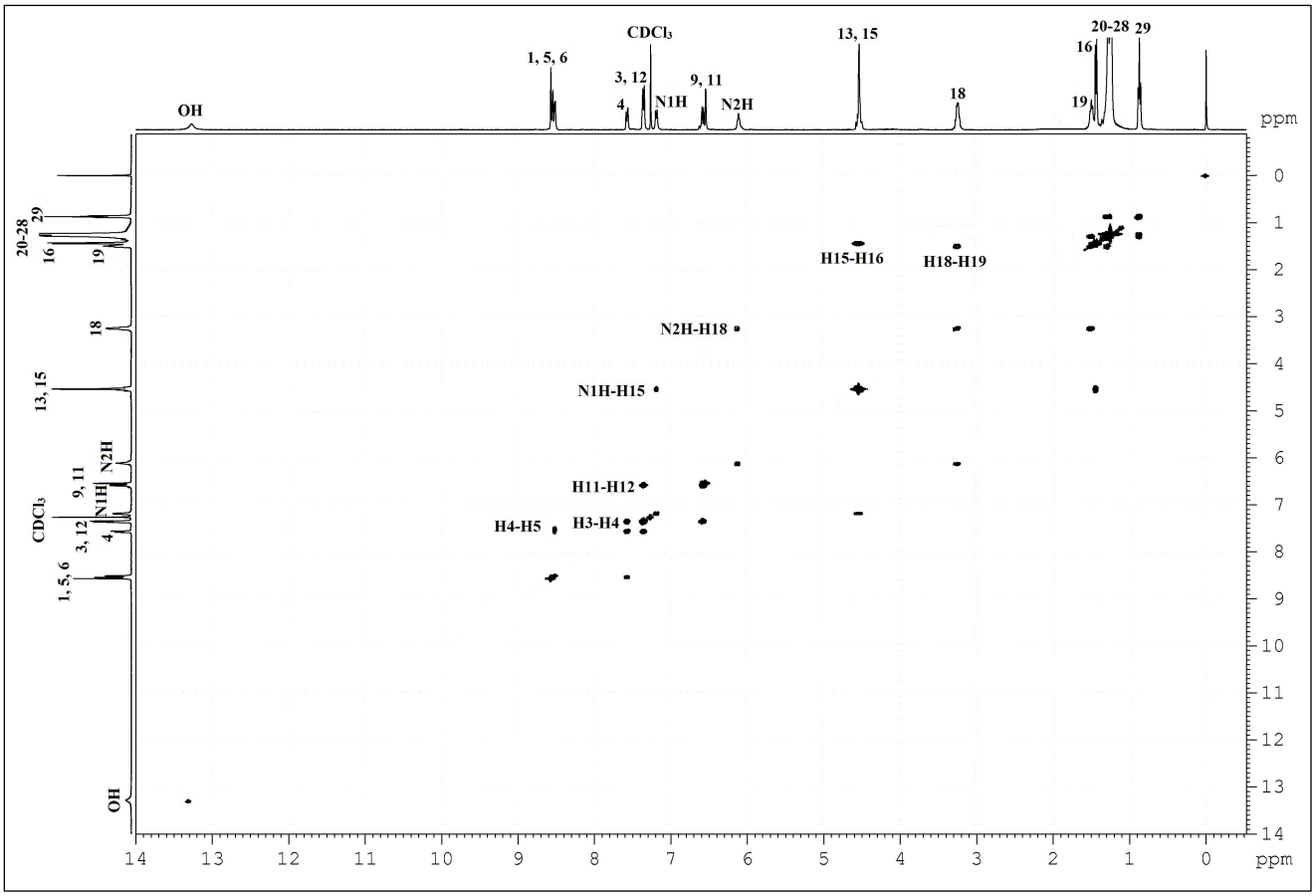

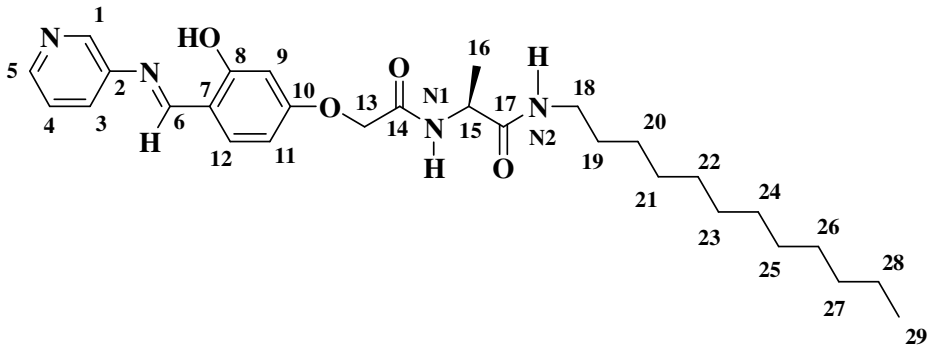

Figure S16. H-H COSY spectrum of compound **1** in $CDCl_3$.

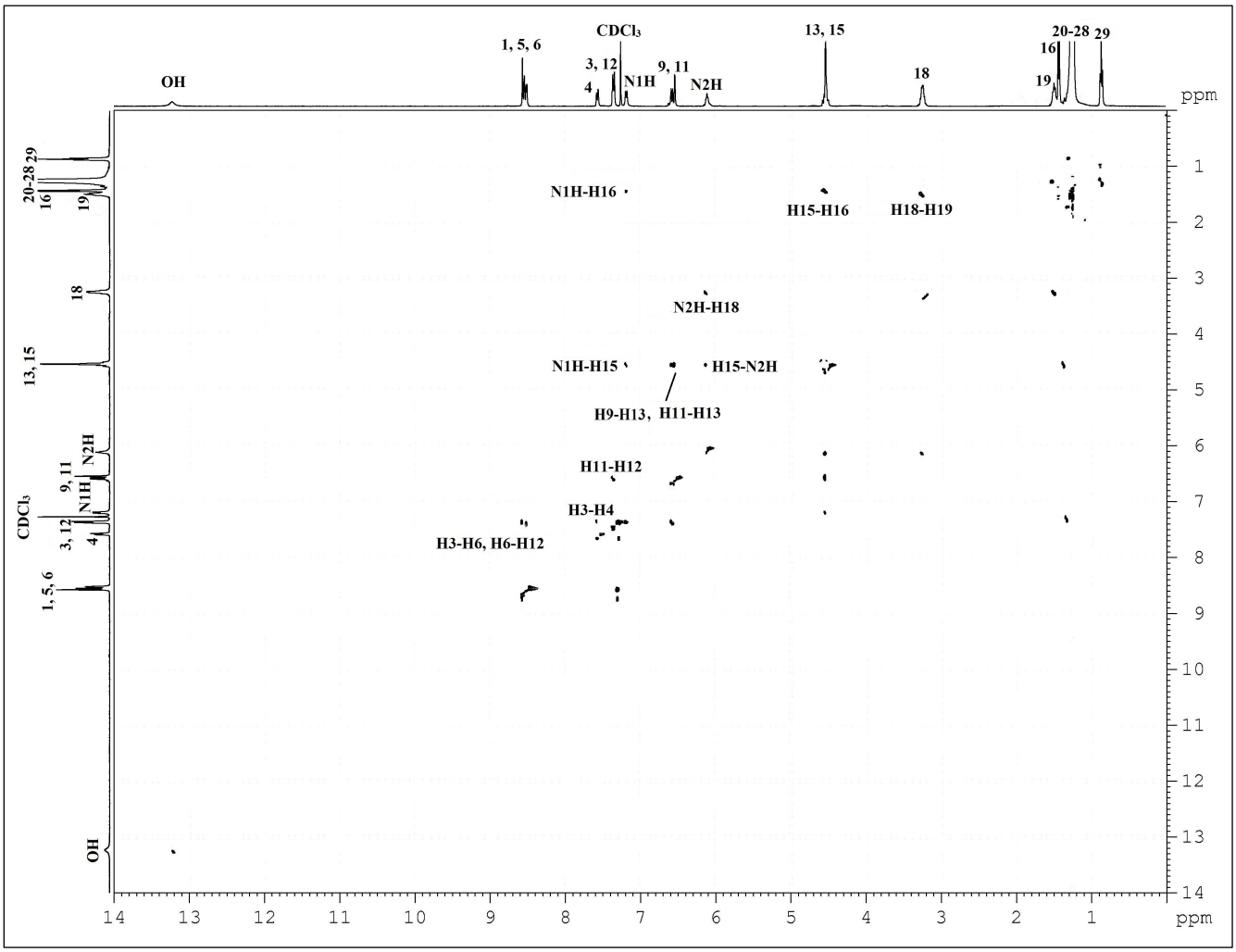

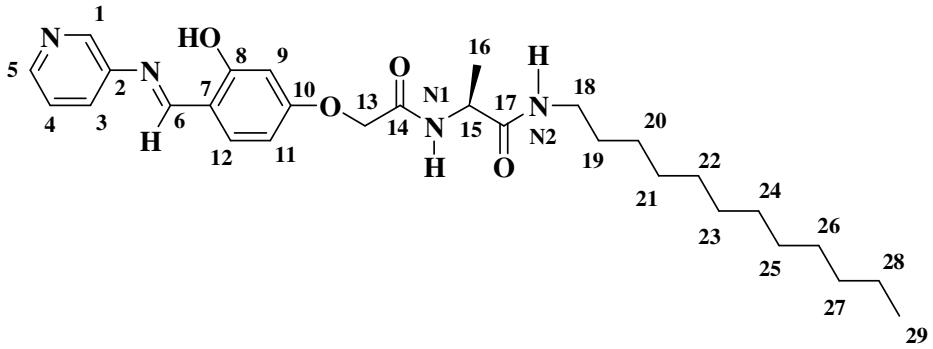

Figure S17. H-H NOESY spectrum of compound **1** in $CDCl_3$.

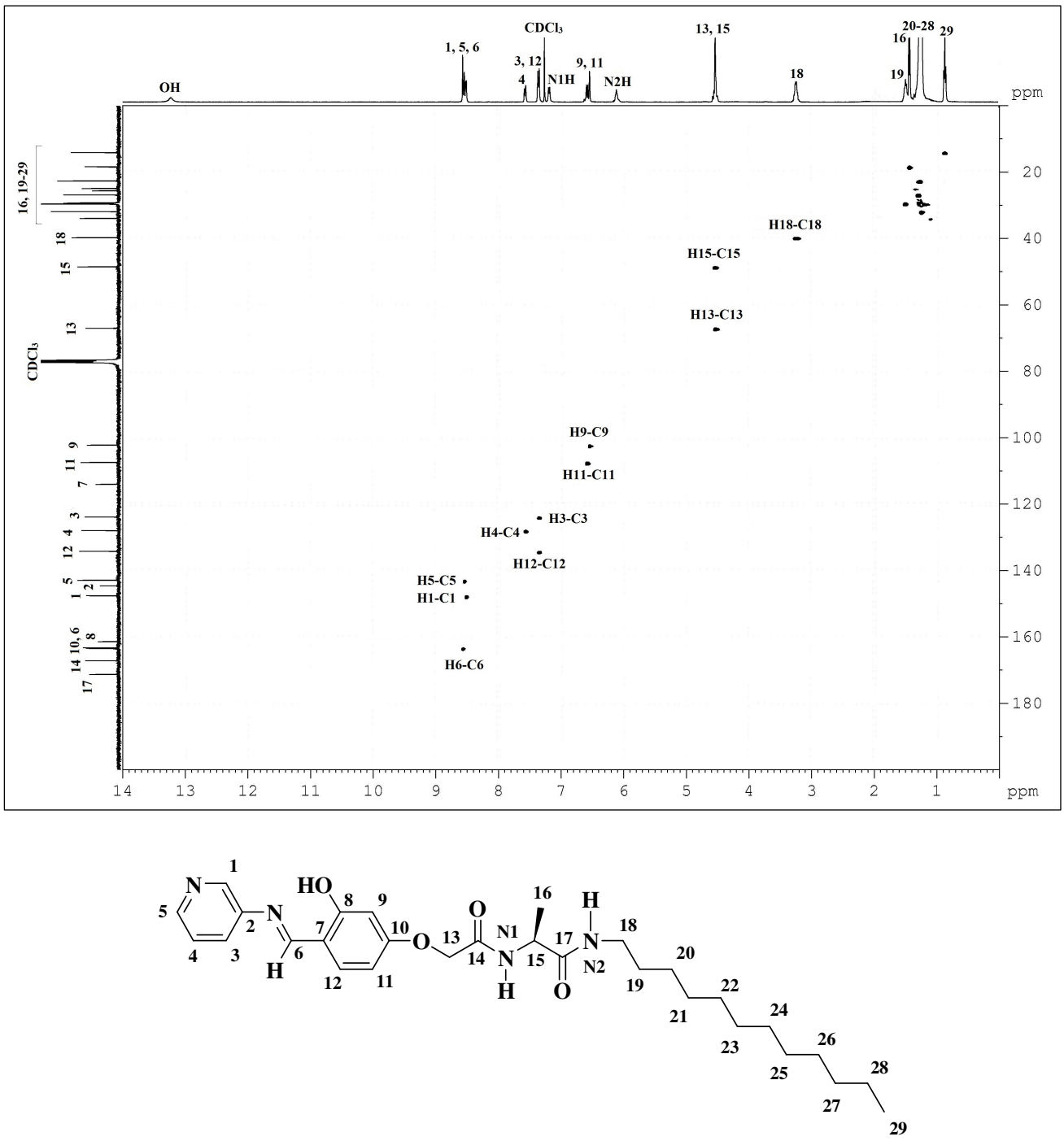

Figure S18. HSQC spectrum of compound **1** in $CDCl_3$.

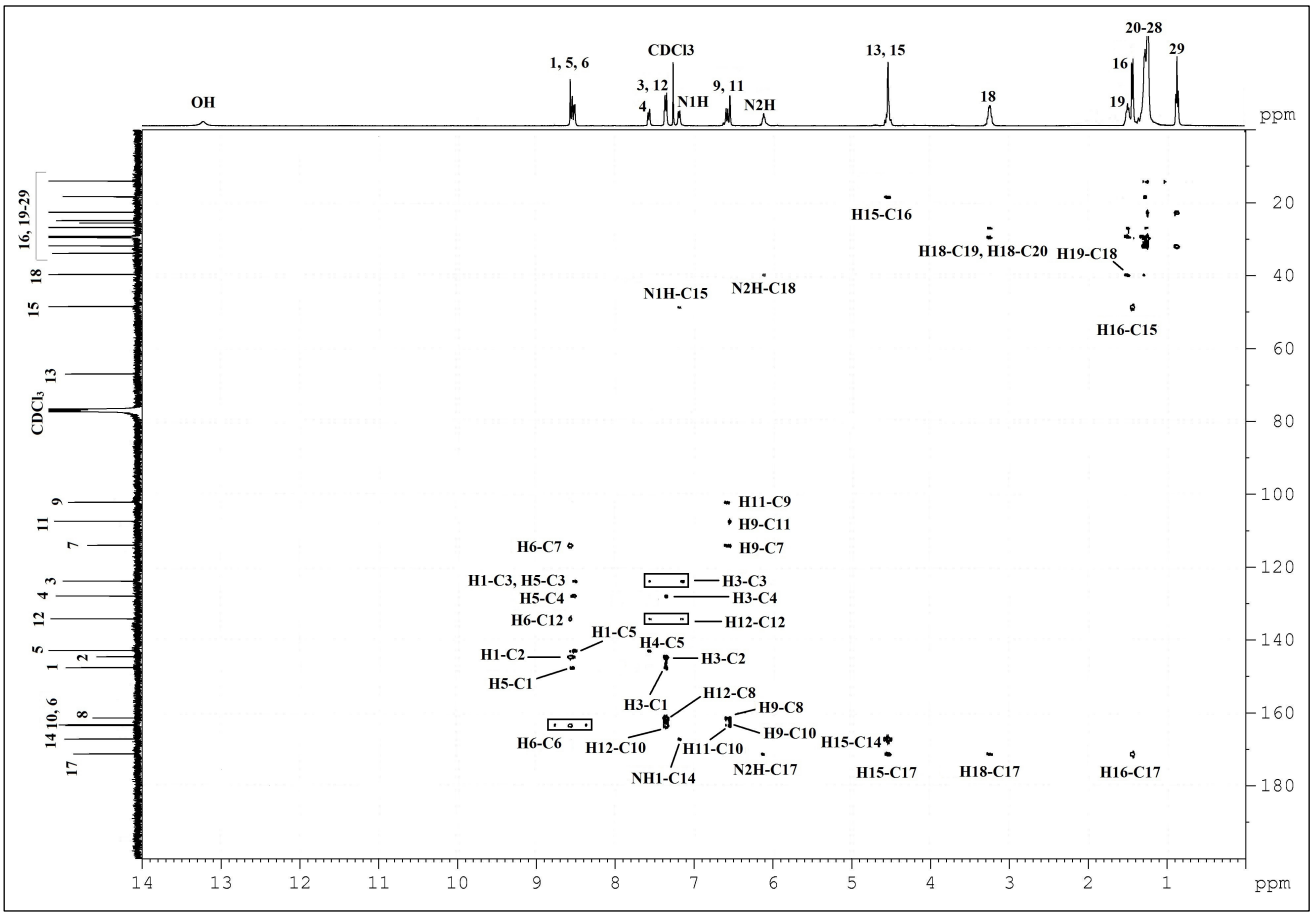

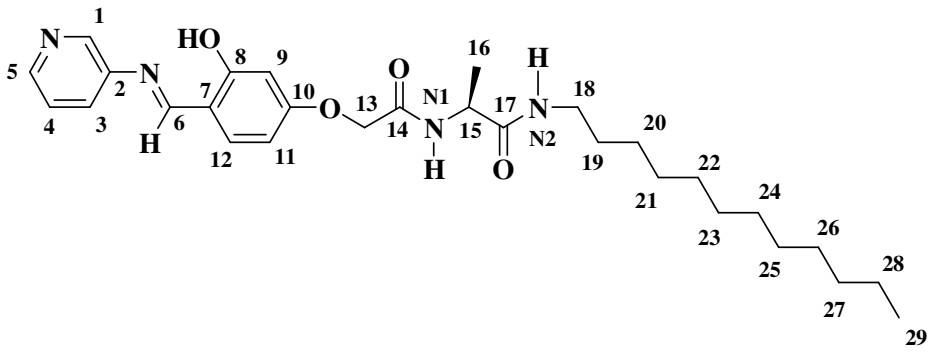

Figure S19. HMBC spectrum of compound **1** in $CDCl_3$.[a]

[a] ^1J correlations sometimes break through filter; show up as multiple cross peaks.[4,5]

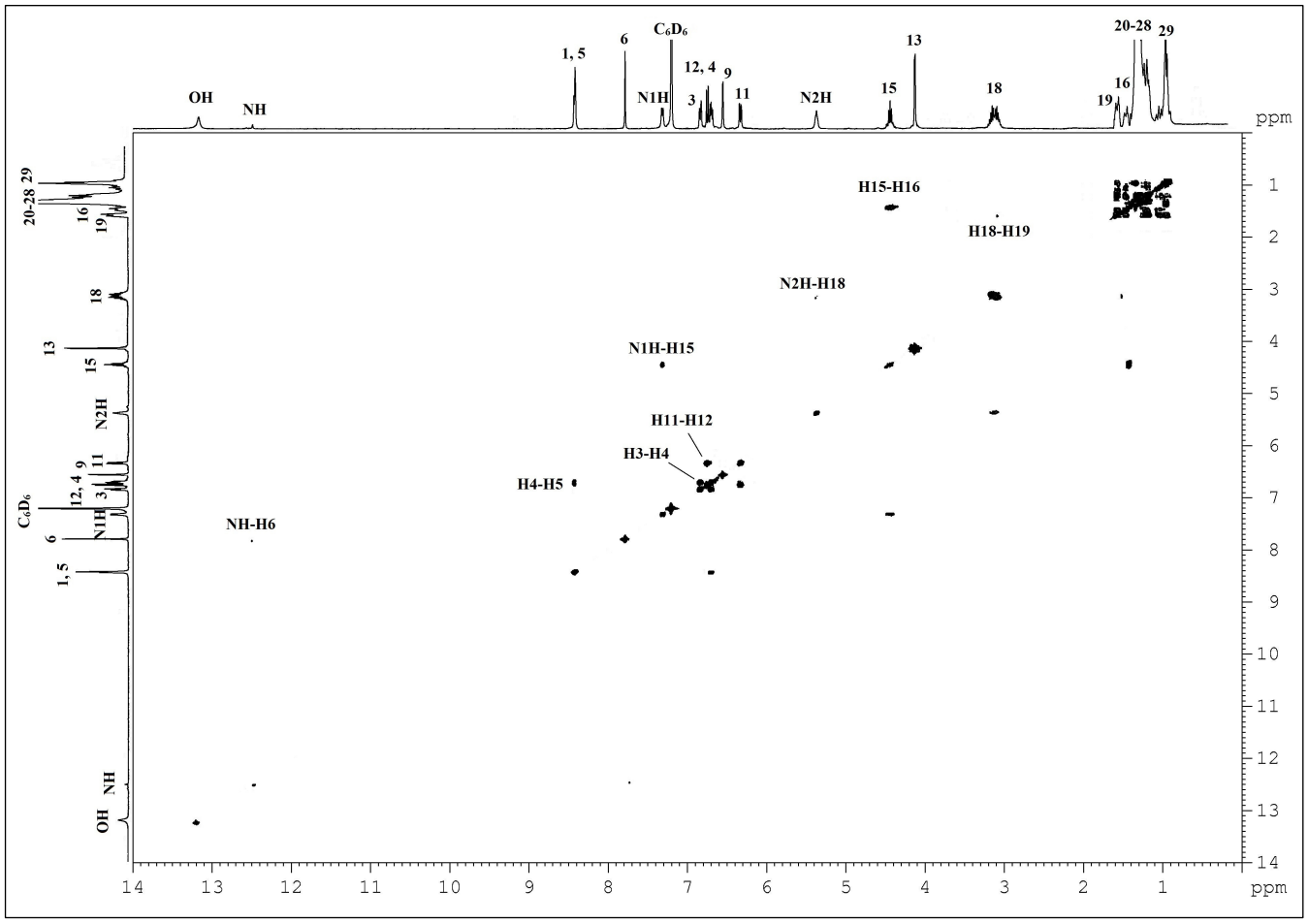

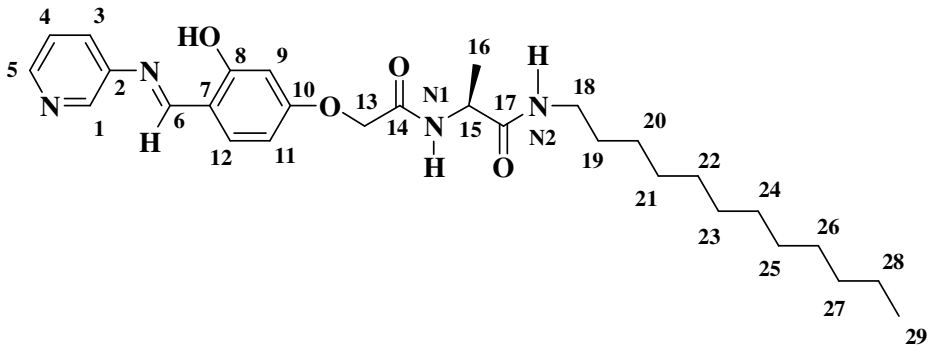

Figure S20. H-H COSY spectrum of compound **1** in C_6D_6.

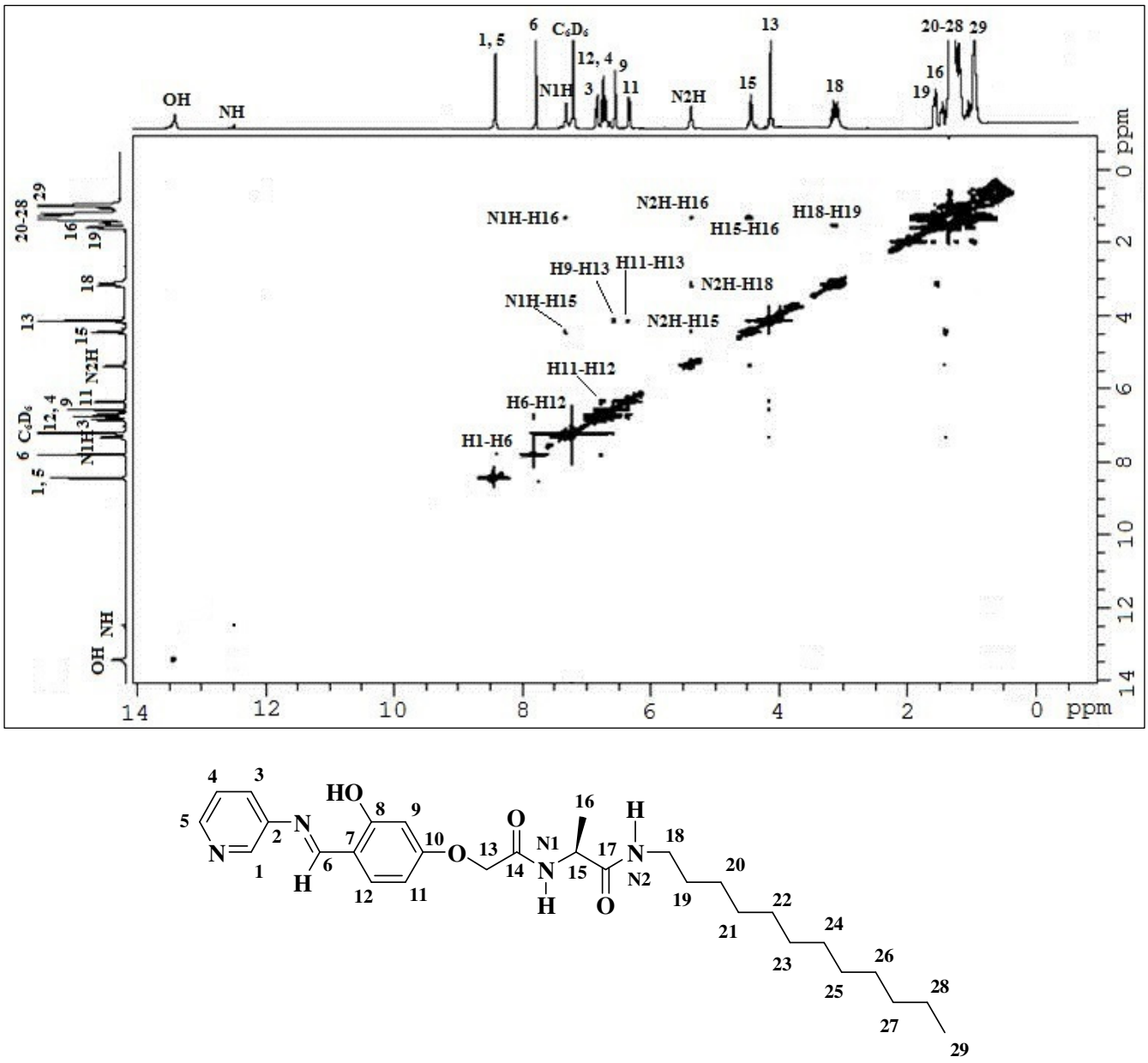

Figure S21. H-H NOESY spectrum of compound **1** in C_6D_6.

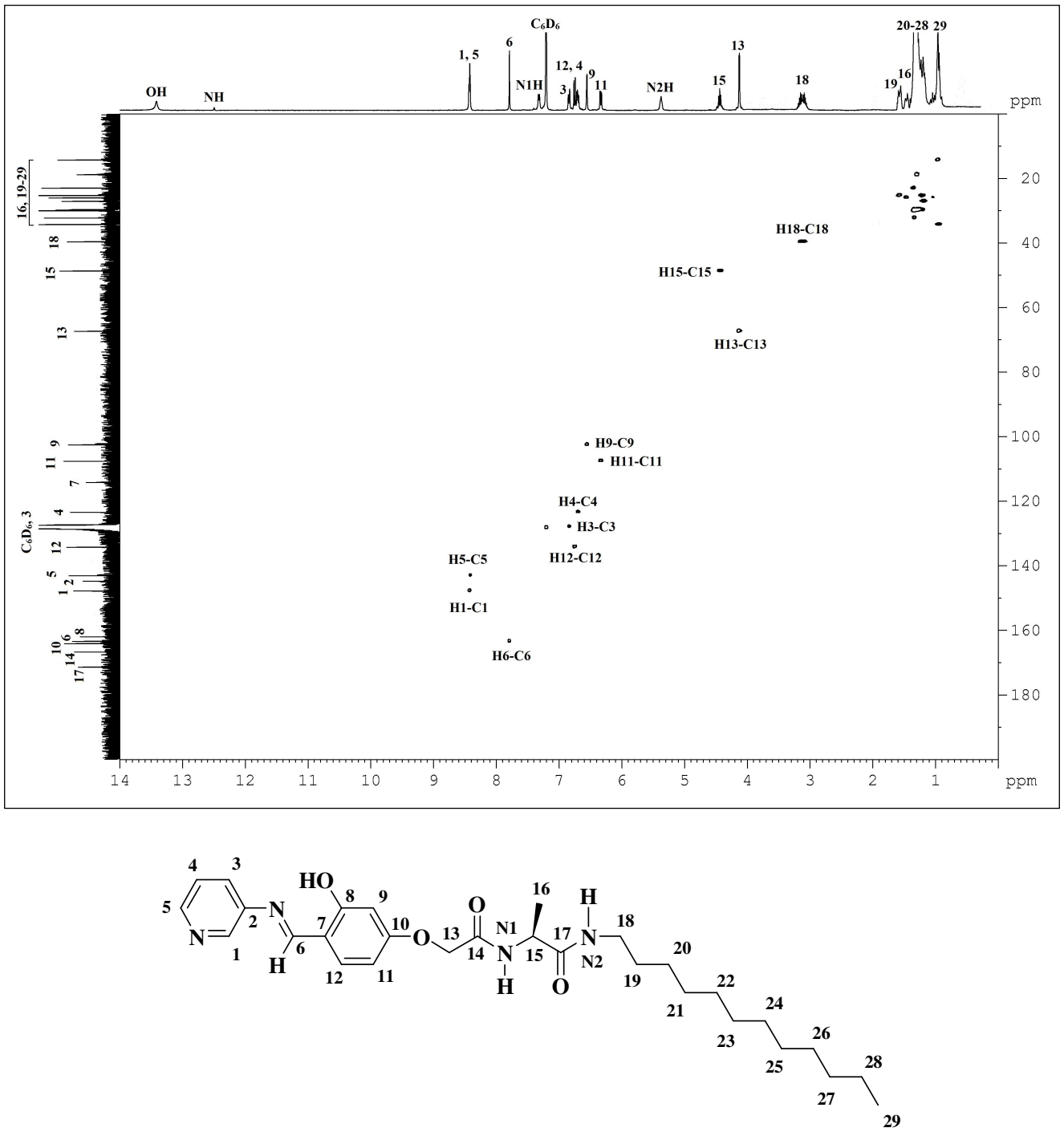

Figure S22. HSQC spectrum of compound **1** in C_6D_6.

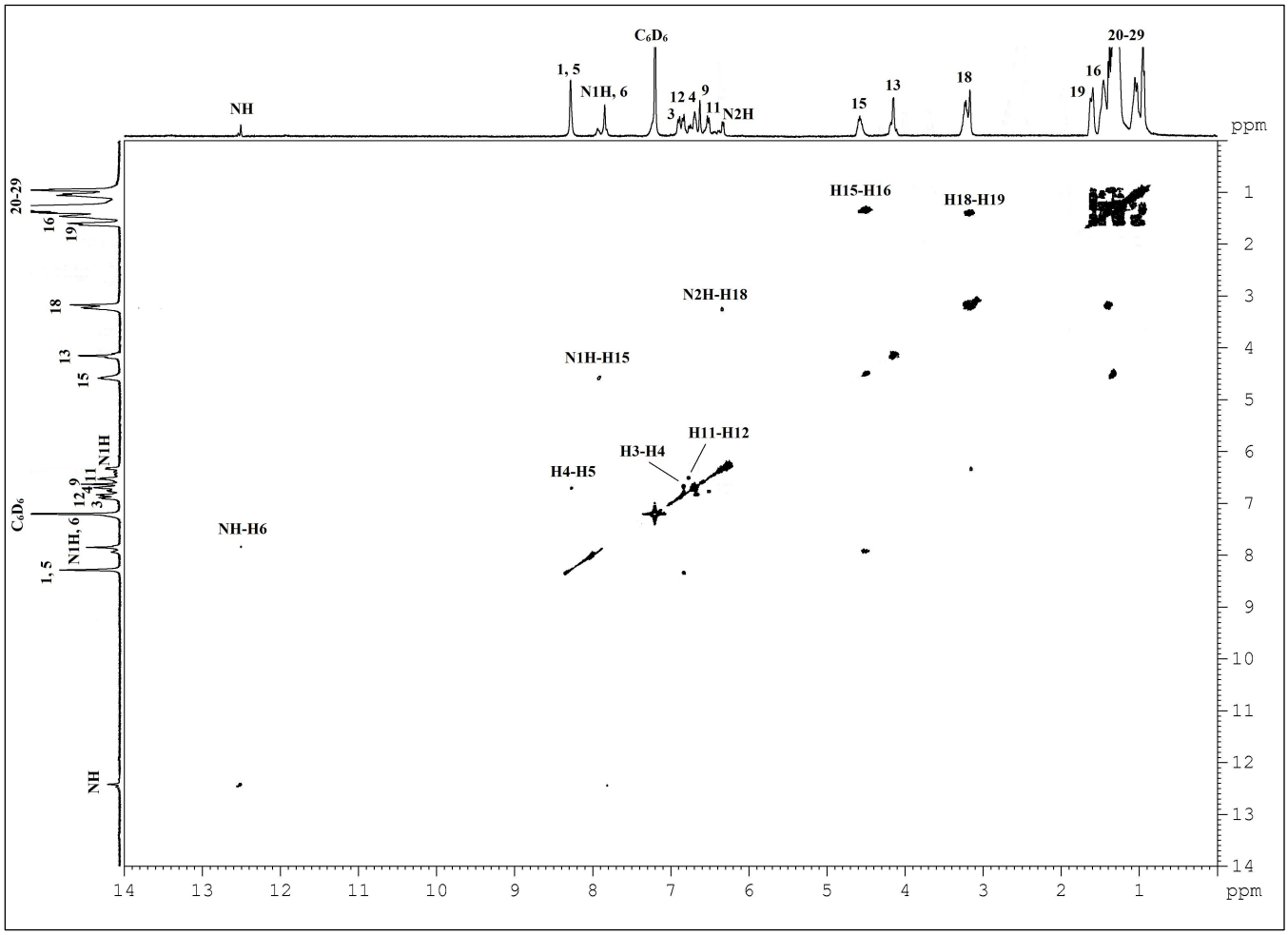

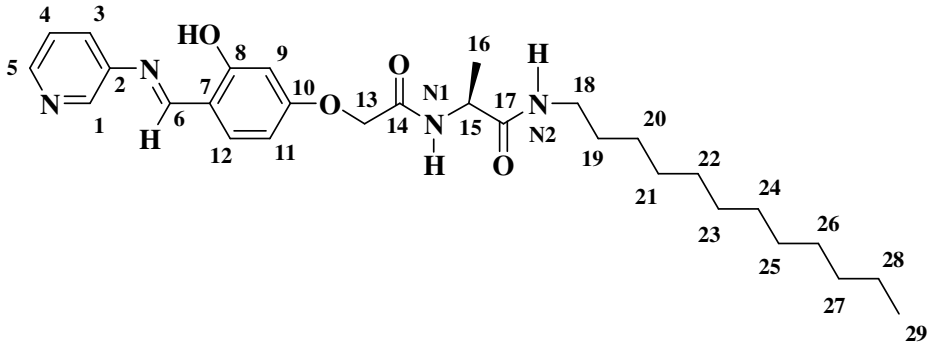

Figure S23. H-H COSY spectrum of Ag^{+} coordination complex of **1** in [D_6]benzene.

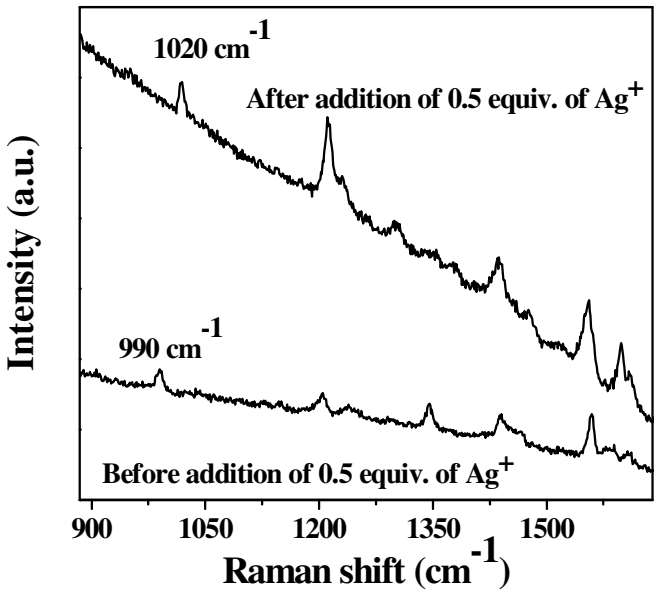

Figure S24. Raman spectra of **1** and its Ag^+-coordination complex in 100:1 toluene/EtOH (v/v).

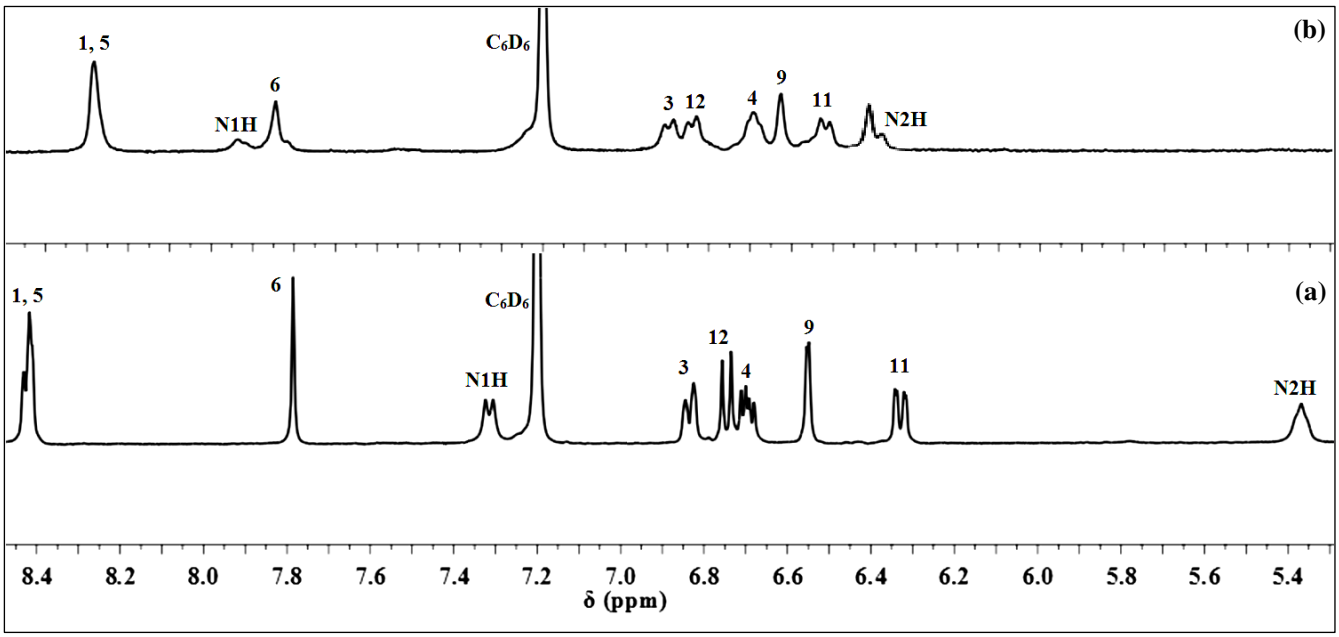

Figure S25. Partial ^{1}H-NMR spectra of (a) **1** (3.9 mM) and (b) its Ag^+-coordination complex in [D_6]benzene in presence of 1% CD_3OD (v/v).

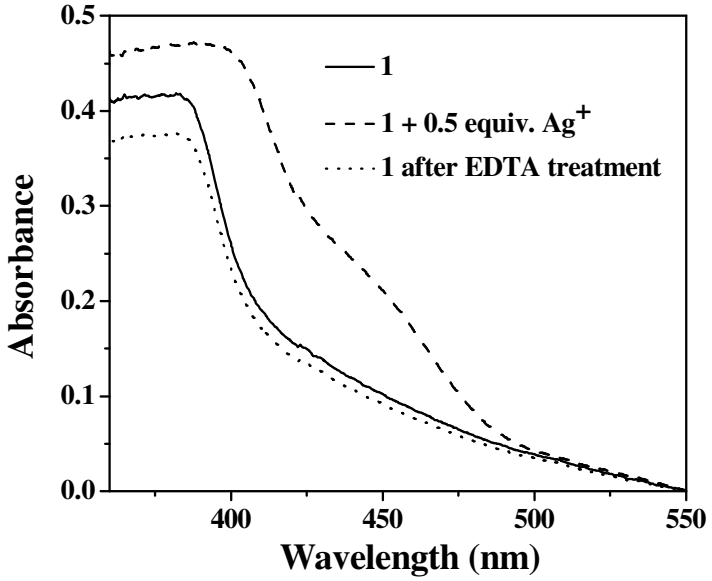

Figure S26. UV-Vis spectra of **1** (0.39 mM), Ag^{+}-coordination complex gel and the residue obtained from the organic layer after treatment with the aq. solution of EDTA (0.4 mM) in 100:1 toluene/EtOH (v/v).

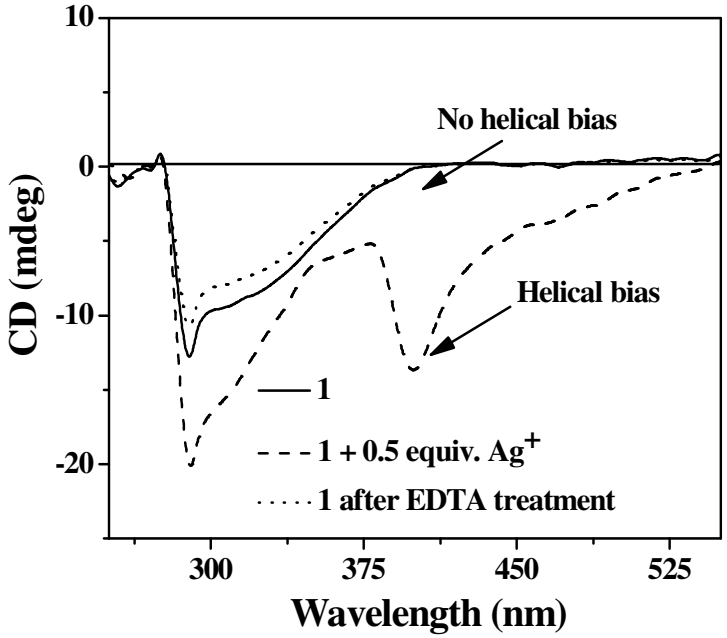

Figure S27. CD-spectra of **1** (0.39 mM), Ag^{+}-coordination complex gel and the residue obtained from the organic layer after treatment with the aq. solution of EDTA (0.4 mM) in 100:1 toluene/EtOH (v/v).

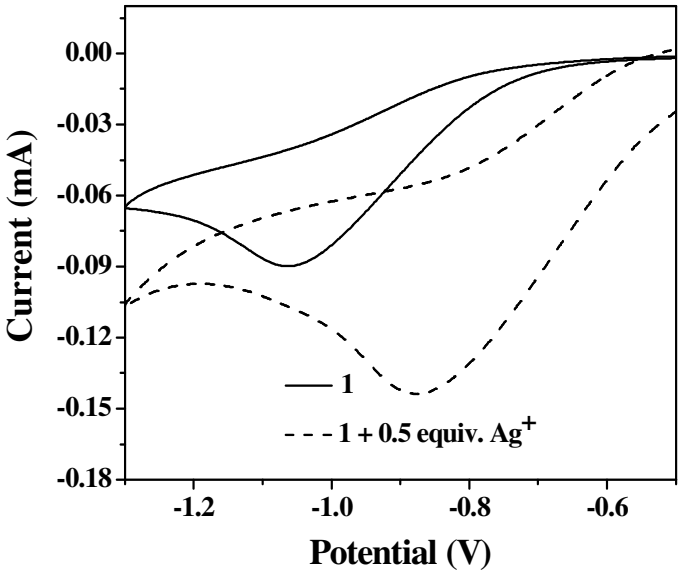

Figure S28. Cyclic voltammetric responses of **1** (3.9 mM) and its Ag^{+}-coordination complex gel on a glassy carbon electrode in 5:1 (v/v) toluene/acetonitrile mixture in presence of 0.1 (M) *n*-$Bu_4N^{+}PF_6^{-}$ as supporting electrolyte at a scan rate of 0.1 V/sec.

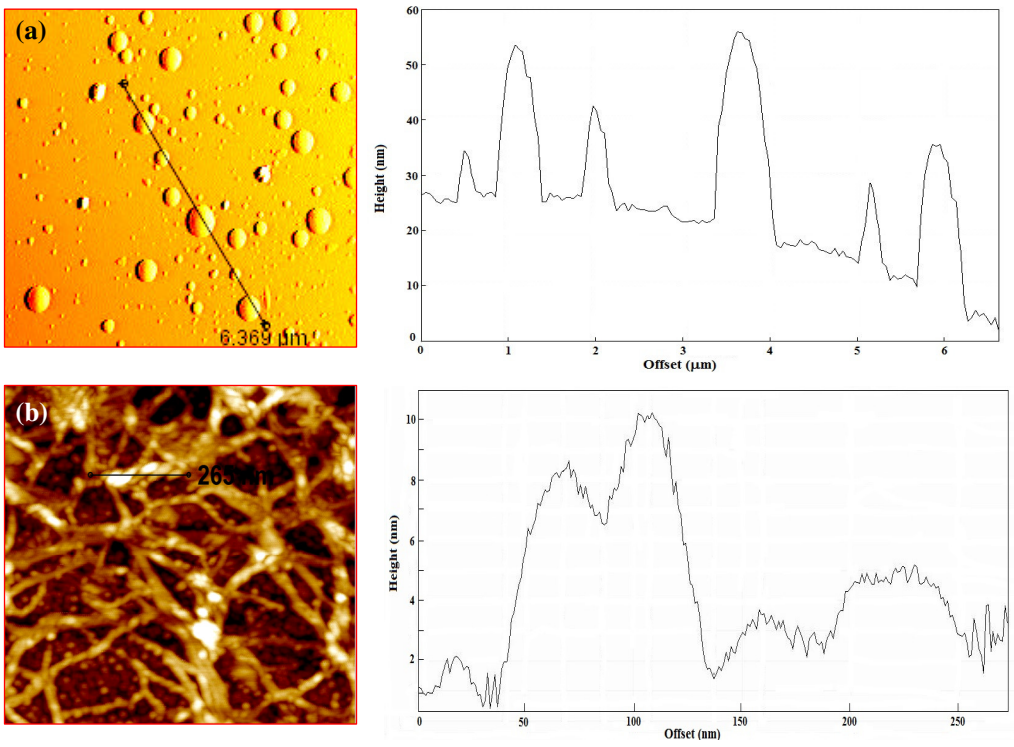

Figure S29. AFM height profiles of (a) **1** and (b) its Ag^{+}-coordination complex in 100:1 toluene/EtOH (v/v).

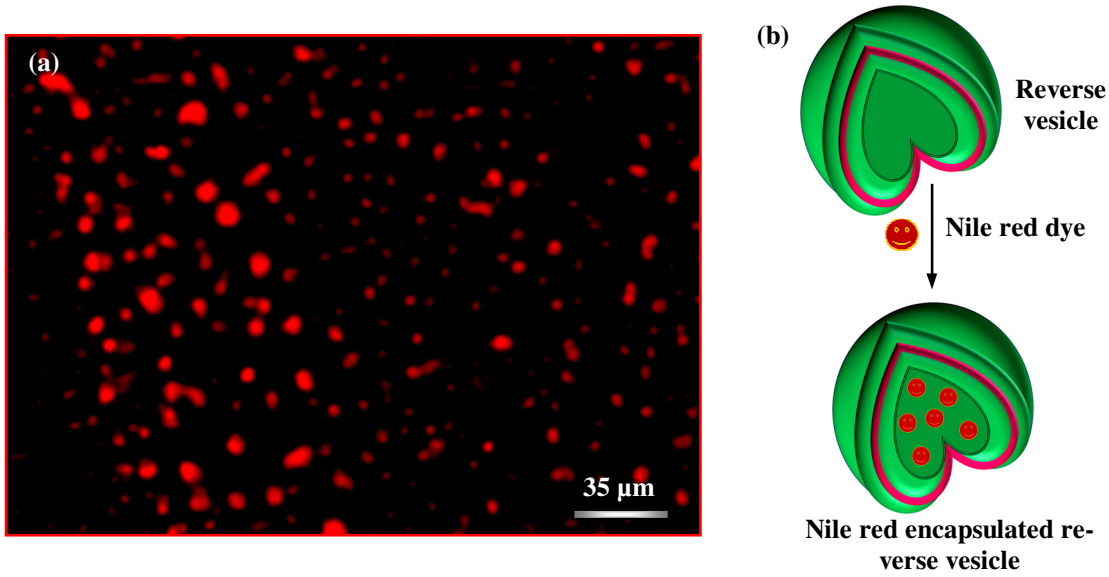

Figure S30. (a) Fluorescence microscopic image of Nile red dye (0.39 mM) encapsulated reverse vesicles of **1** (3.9 mM). (b) A schematic illustration of encapsulation of the hydrophobic Nile red dye molecules inside the hydrophobic cavity of a reverse vesicle of **1** in toluene.

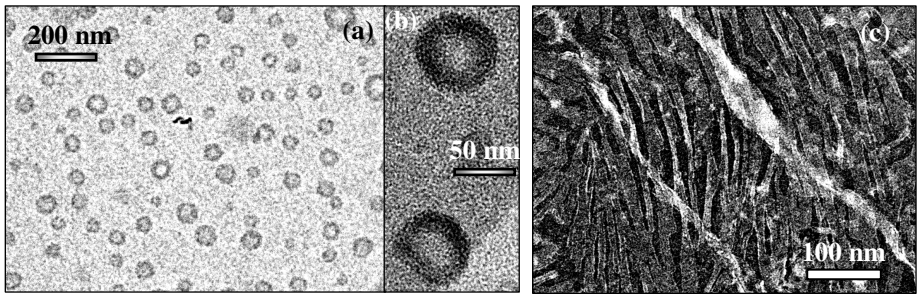

Figure S31. TEM images of (a, b) **1** and (c) its Ag^{+}-coordination complex in 100:1 toluene/EtOH (v/v) using 0.1% uranyl acetate as negative staining agent.

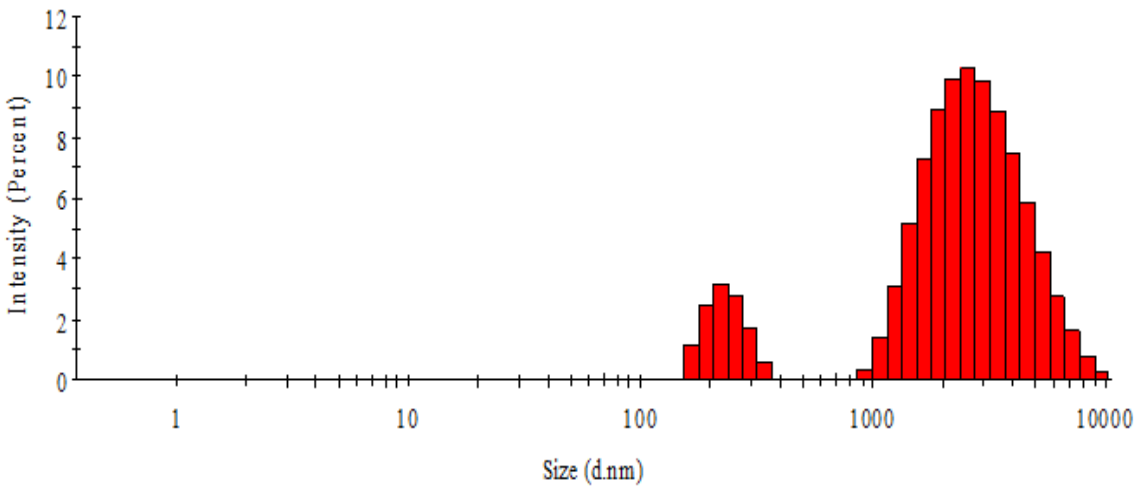

Figure S32. Size distribution of reverse vesicles of **1** (0.39 mM) determined from DLS measurement in 100:1 toluene/EtOH (v/v).

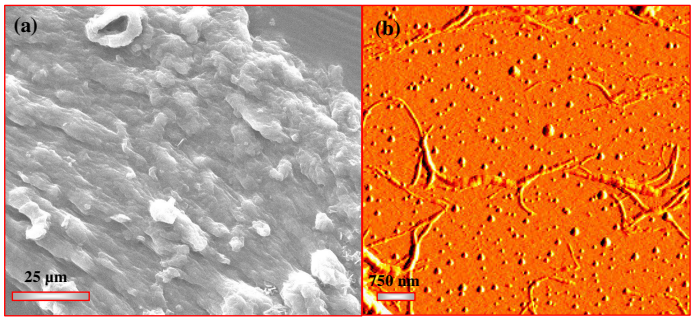

Figure S33. (a) SEM and (b) AFM images of **1** in presence of 0.25 equiv. of Ag^{+} in 100:1 toluene/EtOH (v/v).

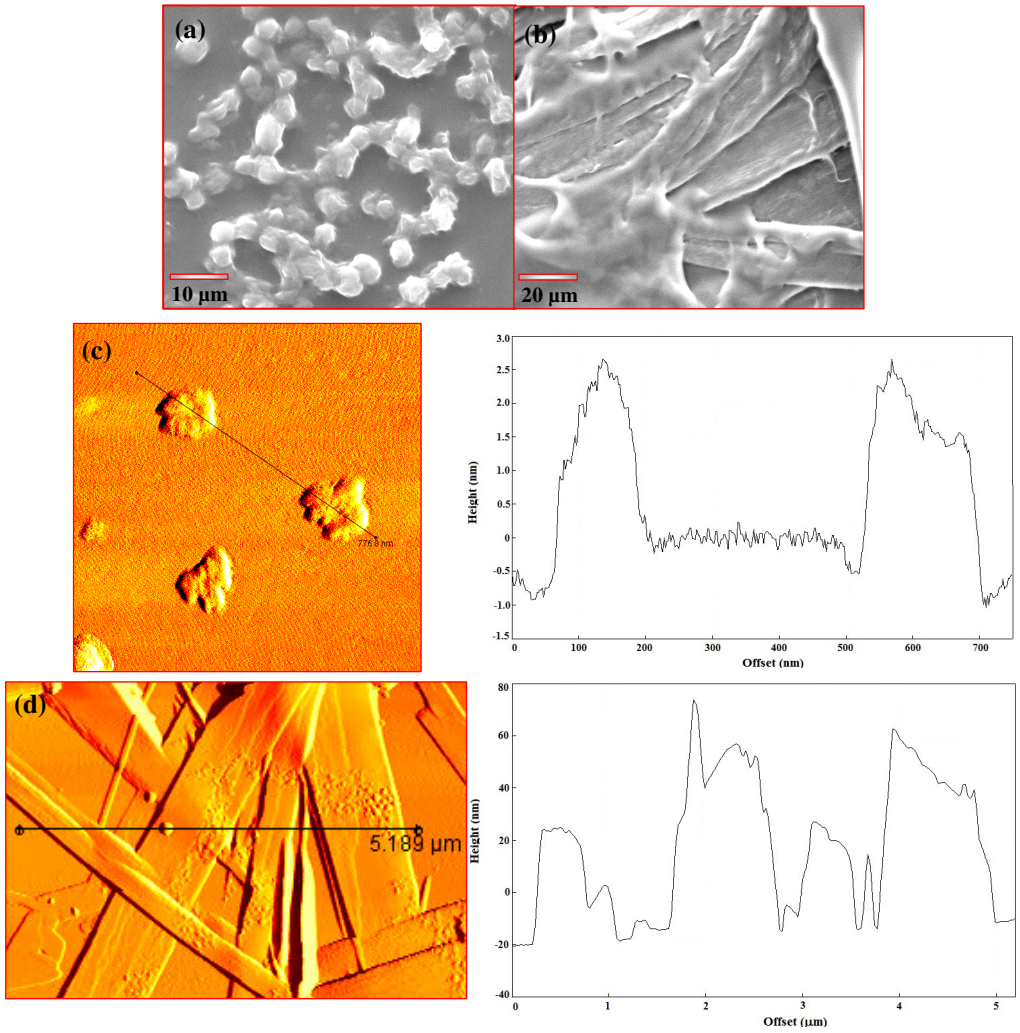

Figure S34. (a and b) SEM and (c and d) AFM height images of **3** and its Ag^{+}-coordination complex in 100:1 toluene/EtOH (v/v).

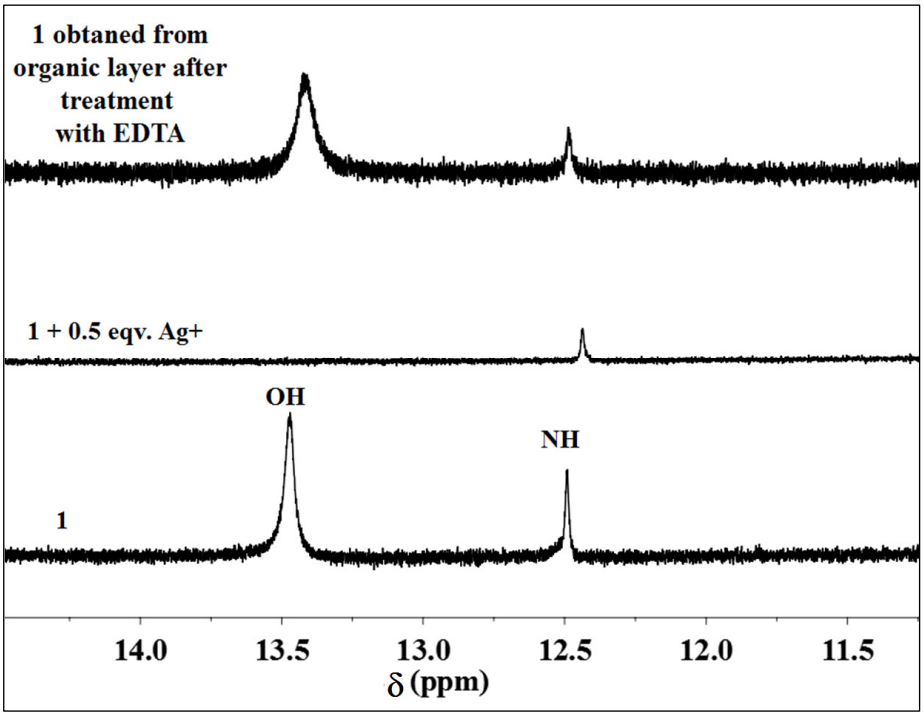

Figure S35. Partial ^{1}H-NMR spectra of **1** (3.9 mM) and its Ag^{+}-coordination complex in [D_6]benzene in presence of 1% CD_3OD (v/v).

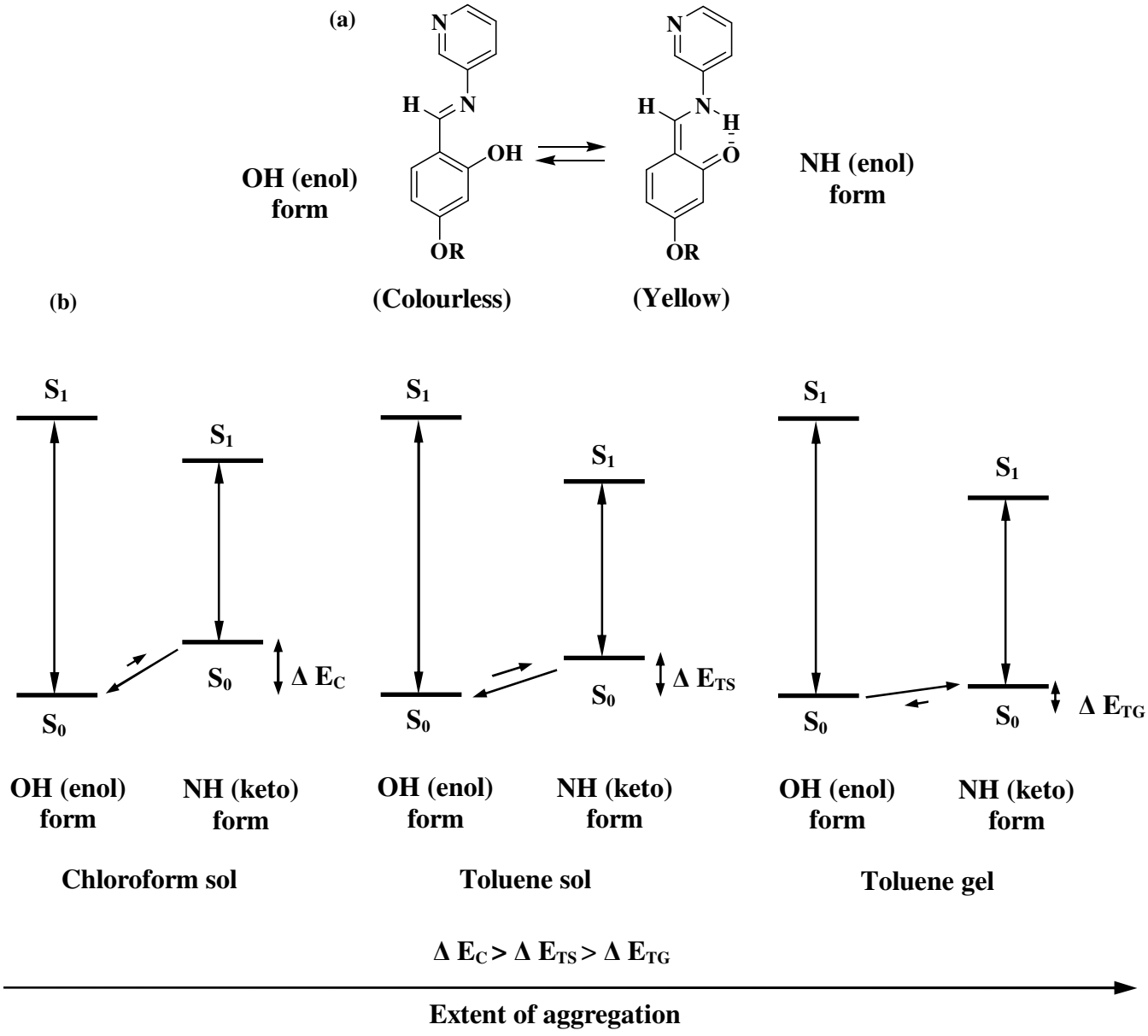

Figure S36. (a) Schematic illustration of keto-enol-tautomerism of **1** and (b) potential energy levels of the OH and NH forms in the chloroform solution, toluene sol and toluene gel.

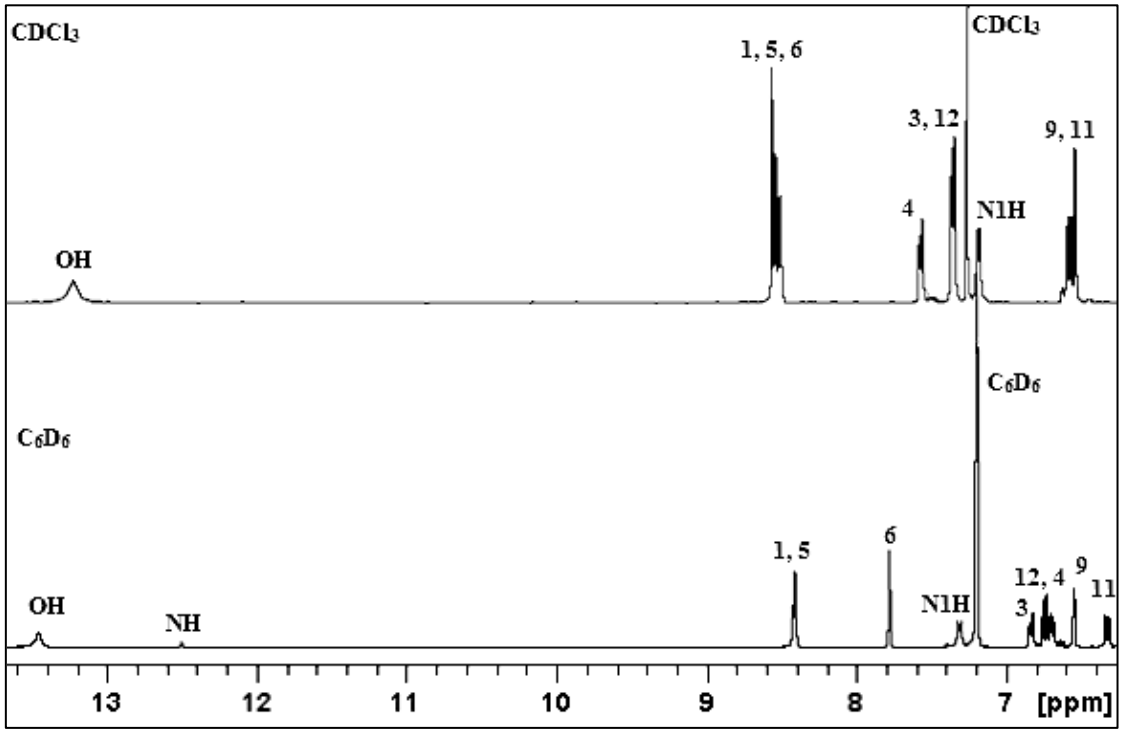

Figure S37. Partial ^{1}H-NMR spectra of **1** in $CDCl_3$ and [D_6]benzene in presence of 1% CD_3OD (v/v) at the concentration of 3.9 mM.

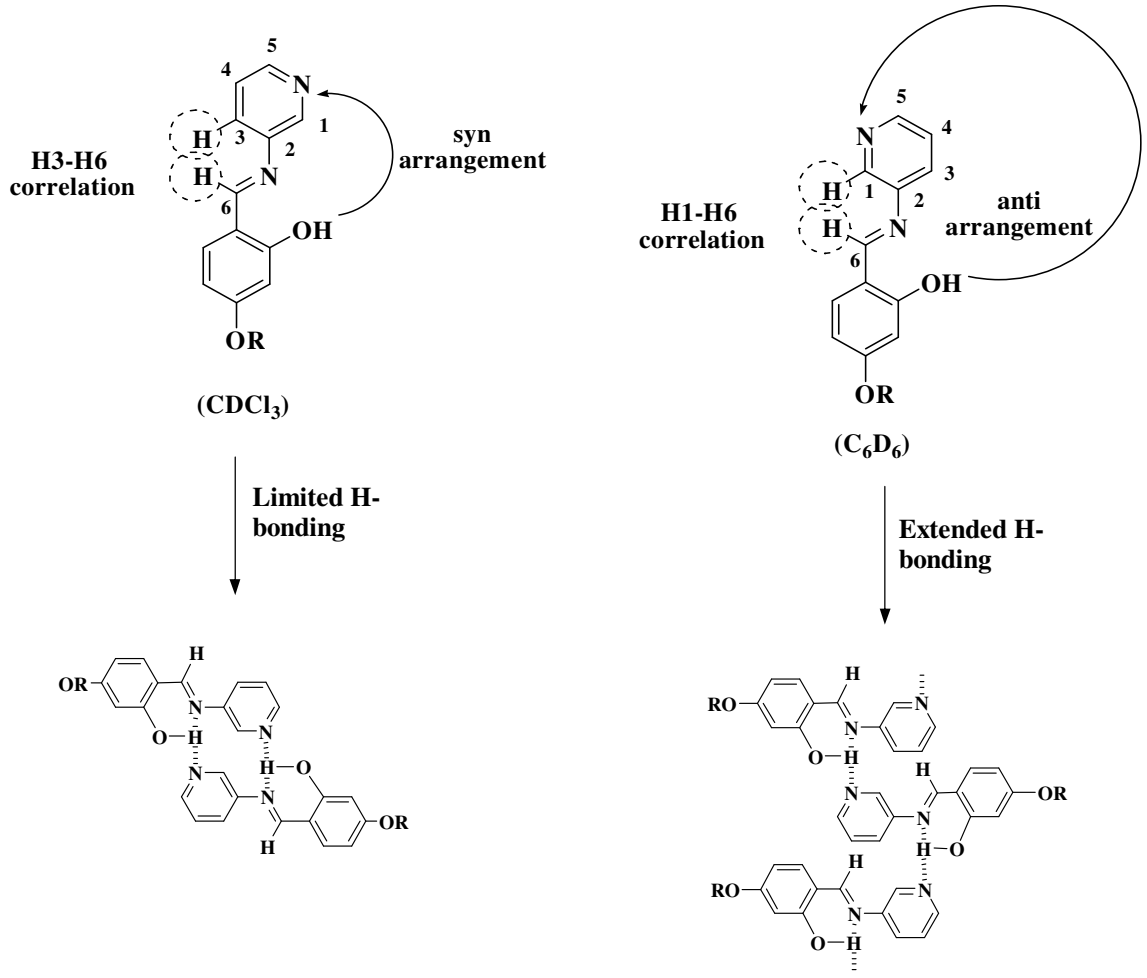

Figure S38. Proposed models of arrangement of pyridyl ring of compound **1** in $CDCl_3$ and C_6D_6.

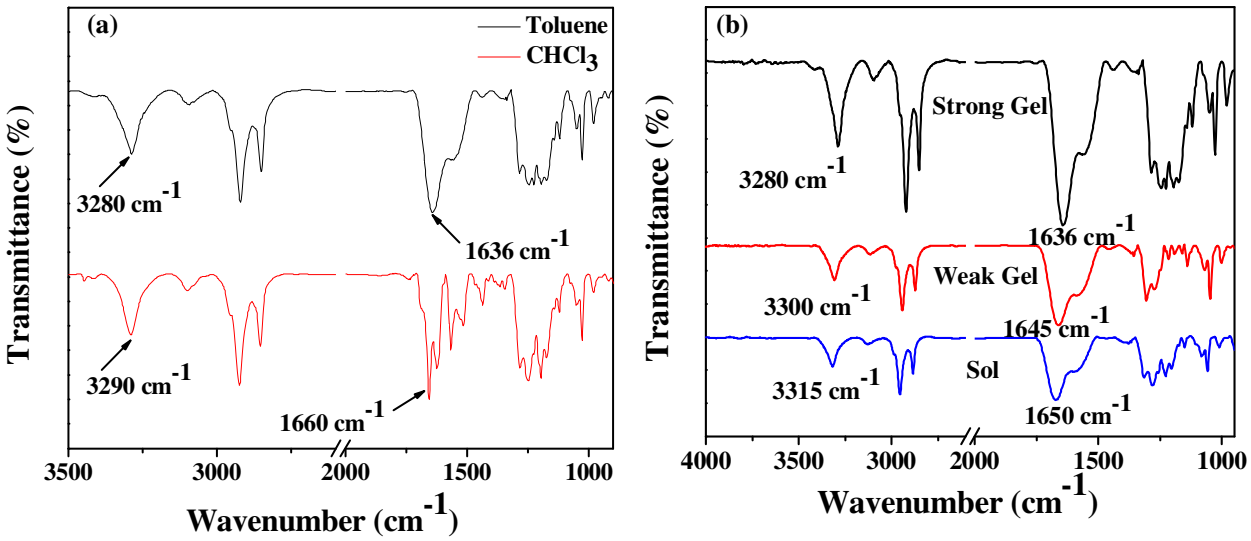

Figure S39. (a) FT-IR spectra of Ag^{+}-coordination complex of **1** in toluene and chloroform; Concentration of compound **1** is 3.9 mM in each case. (b) Concentration-dependent changes in the FT-IR spectra of Ag^{+}-coordination complex **1** of in toluene.[a]

[a] The FTIR-stretching frequencies at 1636 and 3280 cm^{-1} associated with –CONH group in toluene gel of silver coordination complex of **1** shifted to 1660 and 3290 cm^{-1} in chloroform where gelation was not observed (Figure S38a). The shift to higher wavenumber is attributed to the weakening of inter-molecular H-bonding among the –CONH groups.[1,2] Figure S38b shows that the -NH stretching frequency at 3280 cm^{-1} in the "strong" gel (3.9 mM) shifted to 3300 cm^{-1} in the "weak" gel (2 mM) and 3315 cm^{-1} in the "sol" state (1 mM). Thus, shifts of stretching frequencies to higher wavenumbers on dilution indicates a progressive decrease of the inter-molecular H-bonding by the gelators in the self-assembly.[1,2]

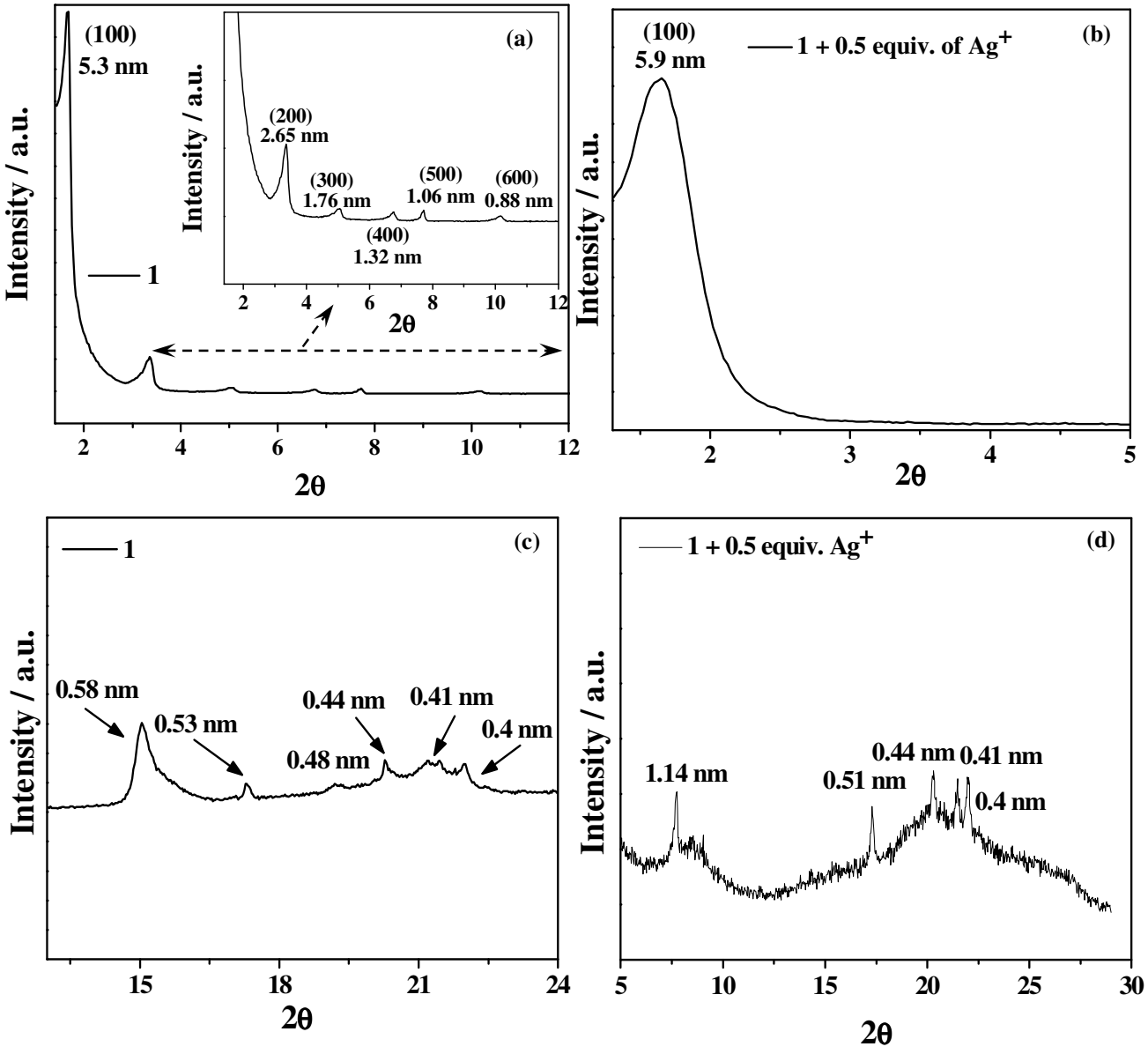

Figure S40. (a and b) Small and (c and d) Wide-angle X-ray diffraction plots of **1** and its Ag^{+}-coordination complex respectively.

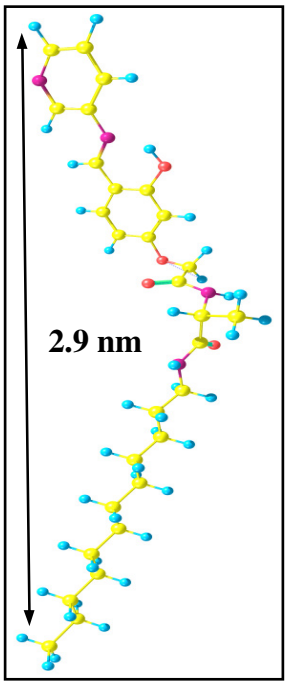

Figure S41. Optimized geometry of **1** using B3LYP/6-31G*.

References.

1. S. Datta, S. K. Samanta and S. Bhattacharya, *Chem. Eur. J.*, 2013, **19**, 11364.

2. S. Datta and S. Bhattacharya, *Chem. Commun.*, 2012, **48**, 877.

3. M. G. Thomas, C. Lawson, N. M. Allanson, B. W. Leslie, J. R. Bottomley, A. McBride and O. A. Olusanya, *Bioorg. Med. Chem. Lett.*, 2003, **13**, 423.

4. D. Ke, C. Zhan, A. D. Q. Li and J. Yao, *Angew. Chem., Int. Ed.*, 2011, **50**, 3715.

5. http://www.chem.umn.edu/groups/taton/chem8361/Handouts/10_17.pdf